



## Review

## Visible-light promoted bimetallic catalysis

Akiko Inagaki<sup>a,b</sup>, Munetaka Akita<sup>a,\*</sup><sup>a</sup> Chemical Resources Laboratory, Tokyo Institute of Technology, R1-27, 4259 Nagatsuta, Midori-ku, Yokohama 226-8503, Japan<sup>b</sup> PRESTO-JST (Precursory Research for Embryonic Science and Technology, Japan Science and Technology Agency), Japan

## Contents

1. Introduction .....	1220
1.1. Visible-light promoted reactions catalyzed by transition metal species .....	1221
1.2. Features of bimetallic systems .....	1221
1.3. Catalytic reactions promoted by visible light .....	1222
2. Catalytic reactions involving electron transfer (A-type transformations) .....	1222
2.1. Hydrogen evolution from H <sup>+</sup> .....	1222
2.2. CO <sub>2</sub> reduction .....	1223
2.3. Pd-catalyzed Sonogashira coupling reaction .....	1226
3. Catalytic reactions involving energy transfer (B-type transformations) .....	1228
3.1. <i>Trans-to-cis</i> isomerization of cyanostilbene .....	1228
3.2. Catalytic olefin dimerization promoted by [(bipy) <sub>2</sub> Ru(μ-BL)PdL <sub>n</sub> ] species .....	1228
3.2.1. Synthesis of heterobimetallic catalysts .....	1229
3.2.2. Spectroscopic and structural characterization of the bimetallic catalysts .....	1231
3.2.3. Selective photocatalytic dimerization of α-methylstyrene promoted by [(bipy) <sub>2</sub> Ru(μ-bpm)PdMe(NCMe)] <sup>3+</sup> <b>44a</b> under visible-light irradiation: catalytic reaction and mechanisms .....	1232
3.2.4. Improvement of the catalytic performance .....	1232
3.2.5. Photocatalytic olefin dimerization by <b>44</b> - and <b>52</b> -type catalysts .....	1236
4. Future prospects .....	1237
Acknowledgements .....	1237
References .....	1237

## ARTICLE INFO

## Article history:

Received 8 October 2009

Accepted 3 November 2009

Available online 12 November 2009

## Keywords:

Visible light

Bimetallic catalyst

Photosensitization

Tris(bipyridyl)ruthenium

Palladium

Catalytic olefin dimerization

## ABSTRACT

Visible-light promoted molecular transformations catalyzed by bimetallic species containing a [Ru(bipy)<sub>3</sub>]<sup>2+</sup> (TB)-like fragment as the photosensitizing unit are reviewed. Catalytic reactions are classified according to the following two criteria: (1) electron transfer (**A**)/energy transfer (**B**) from TB and (2) intra- (**I**) and inter-molecular catalyst systems (**II**). Reactions promoted by electron transfer (**A**) involve reductive processes such as H<sup>+</sup>-reduction giving H<sub>2</sub> and CO<sub>2</sub>-reduction giving CO, which have been extensively studied also by using mononuclear catalysts. The catalytic H<sup>+</sup>- and CO<sub>2</sub>-reductions have been considerably improved by the use of **II-A**- and **I-A**-type bimetallic catalysts, respectively. Furthermore, as recently reported by our research group, photocatalysis is extended to organic transformations, which have been much less explored compared to transformations of small inorganic molecules mentioned above. While Sonogashira coupling is mediated by **II-A**-type catalysts, up-hill *trans-to-cis* isomerization of cyanostilbene and dimerization of α-methylstyrene follow the energy transfer processes (**B**). Thus new aspects of the photochemical bimetallic catalysis have been unveiled as mentioned above but catalyst design is still in its infancy. Continued accumulation of reaction data and mechanism analysis will lead to development of practical bimetallic photocatalysts, which promote unique reactions including up-hill reactions.

© 2009 Elsevier B.V. All rights reserved.

## 1. Introduction

Human beings now confront serious and urgent problems such as global climate variation, environmental pollution, and natural resources depletion, which are mostly derived from consumption

\* Corresponding author.

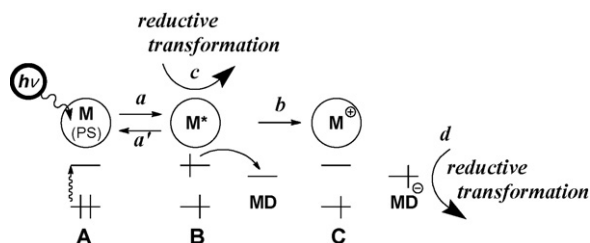
E-mail address: [makita@res.titech.ac.jp](mailto:makita@res.titech.ac.jp) (M. Akita).

of fossil fuel [1]. Under these circumstances, much stress is laid on research to find a clue to such subjects. Above all, utilization of solar energy, which is inexhaustible and clean, has drawn much attention [2]. From this point of view, solar cell and solar water heater are the most popular products already in commercial use; however, ways of utilizing solar energy have been limited to the conversion into electric and thermal energy, and the conversion efficiency is still low to be overcome. It is basically quite difficult to utilize the solar energy owing to its sparse and intermittent supply. On the other hand, plants utilize it in a highly efficient manner through the photosynthesis, in which multi-step processes such as (1) collecting solar energy by the antenna unit, (2) photo-excited energy transfer by chlorophylls, and (3) formation of the charge-separated state are assembled [3]. Combination of these processes with subsequent redox processes should lead to an efficient solar energy conversion into chemical potential energy. Taking into account these points, artificial photosynthesis has been studied intensively in many areas [4].

Research on artificial photosynthesis ranges widely from investigation of elementary processes of the natural photosynthesis to synthesis of chemical substances. Herein discussion will be focused on recent developments of visible-light promoted catalytic reactions using various homogeneous metal catalysts, in particular, (1) *bimetallic catalyst systems containing a  $[Ru(bipy)_3]^{2+}$ -type unit as the photosensitizer and (2) catalytic molecular transformations.*

### 1.1. Visible-light promoted reactions catalyzed by transition metal species

In the field of homogeneous coordination chemistry, research on artificial photosynthesis has been intensively studied mainly by using metal-containing photosensitizers (PS) such as metal-loporphyrins [5] and Ru(II) diimine complexes [6], which show favorable photophysical properties such as long lifetime of the excited state. The research activities have been mainly concentrated on elucidating elementary processes of (1) electron transfer, (2) energy transfer, and (3) formation and deactivation of the charge-separated state. Through the studies, a wealth of important knowledge has been accumulated [7]. However, little attention has been paid to catalytic molecular transformations. A simplified reaction scheme for molecular transformations, in particular, reductive ones, mediated by mononuclear species is summarized in Scheme 1. Photo-excitation of photosensitizer **A** (step *a*) gives an excited species with a high-energy electron (**B**), which may be utilized for reductive transformation directly (step *c*) [8]. Because, however, such direct utilization is usually hampered by backward deactivation (step *a'*), the activated electron is transferred to a mediator (MD) (step *b*), which forms a stable reduced species upon 1e<sup>−</sup>-reduction, and the resultant anionic radical (MD<sup>−</sup>) undergoes reductive transformations (step *d*). For example, in the case of the frequently used MV<sup>2+</sup> (methyl viologen), MV<sup>•+</sup> resulting from the electron transfer from M<sup>\*</sup> is responsible for the subsequent chemical transformations and thus serves as a mediator. (Although details



**Scheme 1.** A simplified reaction scheme for photosensitized reactions promoted by a mononuclear system.

	I : intramolecular system photosensitizing unit (PS) $\rightarrow$ M1 $\xrightarrow{\text{bridging ligand (BL)}}$ M2 $\rightarrow$ reaction center (RC)	II : intermolecular system $\text{M1 (PS)} + \text{M2 (RC)}$
(A) electron transfer system	I-A	II-A
(B) energy transfer system	I-B	II-B

**Scheme 2.** Classification of bimetallic catalysts.

are not described here, a sacrificial electron donor is usually added to fill the lower SOMO in **B** and to suppress the back electron transfer from MD<sup>−</sup> to **C** regenerating **A**. See discussion on Scheme 3.) In such *mononuclear systems*, the two key functions of the catalysis, i.e. light energy collection and molecular transformation, are divided by the metal photosensitizer and the mediator, respectively, or, in some cases, both functions are conducted by a single metal center. Successful examples of mononuclear catalysis [9], including photochemical oxygenation of alkenes with water [10], photocatalytic reduction of CO<sub>2</sub> to CO [11], and photochemical epoxidation of alkenes relevant to the P-450 enzyme [12], were reported during the past decades.

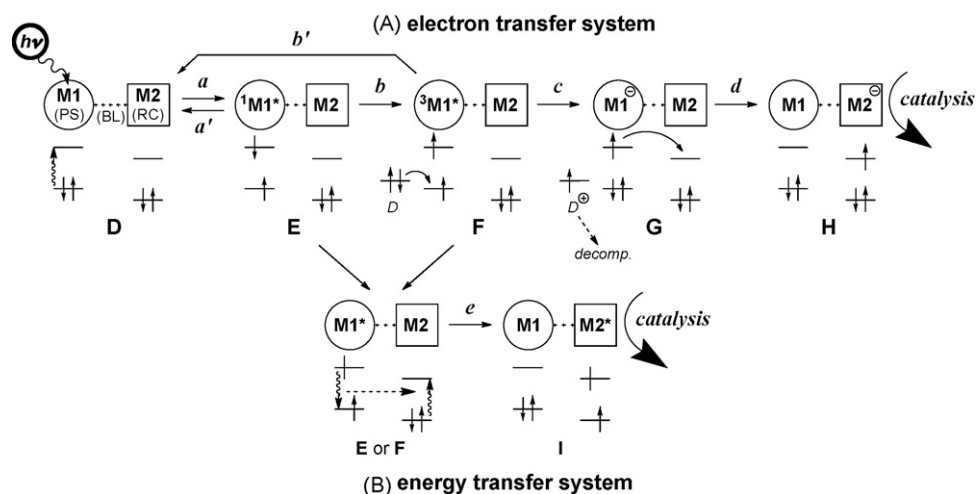
### 1.2. Features of bimetallic systems

A key problem of mononuclear systems is that it is not always easy for a mononuclear catalyst coupled with a simple mediator to promote more complicated chemical reactions such as CO<sub>2</sub> reduction involving multi-electron-reduction and C–C bond formation involving bond breaking and making processes. The previously reported molecular transformations, therefore, have been limited to those mainly based on electron transfer (redox processes).

One of solutions to this problem is to use a transition metal species as the mediator, because transition metal species are known to work as effective catalysts for a variety of molecular transformations, in particular, organic transformations (Scheme 2) [13]. If the two key functions can be divided by two metal centers, we will have many opportunities to construct *bimetallic catalysts*, which are effective for *catalytic molecular (organic) transformation* promoted by visible light. Light energy adsorbed at the photosensitizing metal center (M1(PS)) or photo-excited electron generated at M1(PS) is transferred to the other reactive metal center (M2(RC)) to promote chemical transformations there.

Bimetallic catalysts discussed herein are classified according to the structures and mechanisms into four types (Scheme 2). First, they are classified into two types depending on the structure of the catalyst, i.e. *intramolecular* and *intermolecular* photosensitizing catalysts (**I** and **II** in Scheme 2, respectively). The former (**I**) is a catalyst, which possesses both the light-absorbing, photosensitizing unit (M1(PS)) and the reaction center (M2(RC)) in a single molecule, whereas the latter (**II**) is a mixed system consisting of PS and RC. In the case of **I**, the reaction center (M1(RC)) is linked to the photosensitizing unit (M2(PS)) through an appropriate bridging ligand (BL). The photophysical and photochemical properties and reactivities of the bimetallic catalyst (**I**) can be finely tuned by introduction of substituents onto the ligands attached to M1(PS) and M2(RC) as well as the bridging ligand (BL), but synthesis of multi-functional bimetallic catalysts is essential and sometimes troublesome. On the contrary, the construction of *intermolecular* system (**II**) is much easier, because it can be generated by simply mixing the two components.

Photosensitizing catalytic reactions are further classified into electron-transfer system (**A**) and energy-transfer system (**B**). Fea-



**Scheme 3.** Electron transfer and energy transfer processes based on bimetallic systems.

tures of the bimetallic photochemical systems are illustrated in Scheme 3 for a system containing a  $[\text{Ru}(\text{bipy})_3]^{2+}(\text{TB})$ -like M1 fragment, and electronic configuration of each state is also indicated. In this review article, the  $[\text{Ru}(\text{bipy})_3]^{2+}$  fragment is abbreviated as TB.

In the electron-transfer system (**A**), irradiation of the photosensitizing M1(PS) part in a bimetallic catalyst **D** causes excitation of a HOMO electron to an excited level (MLCT in the case of TB) to form the excited species **E** (step *a*). While **E** can serve as a reductant (by the action of the higher SOMO electron) as well as an oxidant (by the action of the lower SOMO electron), subsequent processes will be explained with the emphasis on the former reductive process. The resultant excited electron can be transferred to the second metal center. But the lifetime of the singlet excited state **E** is too short to undergo electron transfer and **E** is usually deactivated to regenerate **D** (step *a'*). In the case of TB (see below), however, intersystem crossing spontaneously occurs in an almost quantitative quantum yield to give the triplet species **F** (step *b*), which has a lifetime of ca. 1  $\mu\text{s}$  (step *b'*: slow) long enough for a further chemical process. In the presence of an externally added sacrificial electron donor (**D**; tertiary amines are frequently used), subsequent electron transfer from **D** to the lower SOMO gives the negatively charged species **G** (step *c*) [14]. If the LUMO level of M2(RC) is lower than the SOMO level of M1(PS)<sup>−</sup>, further exothermic electron transfer from PS to RC takes place to form another negatively charged species **H** (step *d*), where the transferred electron is located on RC and a reductive chemical transformation can be initiated there [15]. The reaction sequence contains two electron transfer processes indicated by the curved arrows. **D** is essential not only for the electron transfer to **F** but also as an electron source for catalytic reductive transformations. Thus the efficient electron relay from the sacrificial electron donor **D** to the second metal center (M2(RC)) through the M1(PS)<sup>−</sup> species **G** can lead to unique photochemical catalysis at M2(RC).

In the energy-transfer system (**B** in Scheme 3), energy gained at M1(PS) (**E** or **F**) is transferred to M2(RC) to form **I** containing the excited state of RC (RC\*; step *e*), which can initiate a catalytic reaction. In this system, no sacrificial reagent is required, because the energy is provided from a light source continuously. The two processes, **A** and **B**, therefore, can be discriminated by detection of decomposition products of  $\text{D}^{+\bullet}$ .

Photo-chemical and -physical features of  $[\text{Ru}(\text{bipy})_3]^{2+}$  (TB), which is used as the photosensitizer in the catalytic reactions described in the following sections, will be briefly summarized here. Since the utility of TB as a photosensitizer was recognized in 1970s [16], it has become one of popular photosensitizers by

virtue of the following favorable photo-chemical and -physical properties.

- (1) TB shows an intense visible absorption ( $\lambda_{\text{max}} = 450 \text{ nm}$ ;  $\epsilon = 1.5 \times 10^4 \text{ M}^{-1} \text{ cm}^{-1}$ ), the envelope of which is extended to ca. 550 nm. The absorption area is wide enough to collect solar energy (visible light) in an efficient manner.
- (2) Intersystem crossing (included in step *b* in the bimetallic mechanism ( $\text{E} \rightarrow \text{F}$ )) is very fast (rate constant =  $10^{12} \text{ s}^{-1}$ ) and its quantum yield is almost unity, as described above. This means that the energy stored in the excited species **E** is not lost by reverting to **D** (step *a'*) but is stored as the form of **G/H**. Furthermore, because the lifetime of the triplet excited state **F** ( $\sim 1 \mu\text{s}$ ) is longer than the timescale of most chemical reactions (ns– $\mu\text{s}$ ), **F** has many chances to interact with other components via the effective electronic relay (e.g.  $\text{F} \rightarrow \text{H}$  or **I**) and the stored energy can be utilized at M2(RC).

### 1.3. Catalytic reactions promoted by visible light

Substrates of catalytic reactions discussed herein range from small inorganic molecules (e.g.  $\text{H}_2$  and  $\text{CO}_2$ ) to unsaturated organic molecules (e.g. alkene and alkyne). The catalytic reactions can be classified into two categories **A** and **B** as mentioned above. Much attention has been paid to reductive transformations based on **A**, in particular,  $\text{H}_2$  evolution from water ( $\text{H}^+$ -reduction) and  $\text{CO}_2$ -reduction relevant to the energy and environmental issues, respectively. By contrast, little attention has been paid to organic transformation, before we reported coupling reactions of unsaturated hydrocarbons (Section 3.2) [17], which proceeds via **B**. In the following sections, recent studies on catalytic transformations will be reviewed according to the classification, i.e. electron/energy transfer.

## 2. Catalytic reactions involving electron transfer (A-type transformations)

In this section, discussion on two reductive transformations of small inorganic molecules ( $\text{H}^+$  and  $\text{CO}_2$ ) will be followed by organic transformations.

### 2.1. Hydrogen evolution from $\text{H}^+$

Hydrogen is expected to be a next-generation energy carrier [18]. For hydrogen evolution from water, the following two meth-

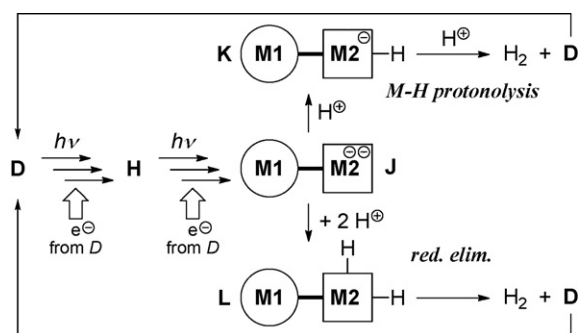
ods are feasible; one is water splitting giving  $\text{H}_2$  and  $\text{O}_2$ , and the other is reduction of  $\text{H}^+$  giving  $\text{H}_2$ . Both reactions are up-hill reactions and, therefore, require injection of energy. Utilization of light energy for the up-hill reactions is a solution. Besides the water splitting promoted by heterogeneous photocatalysts based on metal oxides dispersed on semiconductor particles [19],  $\text{H}^+$ -reduction has been extensively studied in the field of coordination chemistry. Representative examples are summarized in Table 1.

The basic concept for photocatalytic  $\text{H}^+$ -reduction was already established by Lehn in 1970s [20b], who reported the mixed catalyst system consisting of TB ( $\text{M1(PS)}$ ),  $[\text{Rh}(\text{bipy})_3]^{3+}$  ( $\text{M2(RC)}$ ), triethanolamine (TEOA; sacrificial electron donor), and  $\text{K}_2\text{PtCl}_4$  [21]. TON of 77 during 6 h irradiation was achieved. Lehn's system is regarded as a **II-A** type catalyst system, although the role of  $\text{K}_2\text{PtCl}_4$  giving colloidal Pt was not fully clarified [22].

The idea of bimetallic systems originates from combining the photosensitizing TB species with a second metal catalyst ( $\text{M2}$ ), which is capable of  $\text{H}_2$ -formation from a hydride intermediate [24]. Reactions of intermolecular systems (**II**) involve collision processes of the substrates, which determine the efficiency of electron transfer (as a consequence catalytic activity) and are hard to be controlled, whereas, for intramolecular systems (**I**), such a problem does not occur because of arrangement of the two metal centers being fixed and, as a result, it is expected that energy/electron transfer would be more efficient. Catalytic activity of the latter system, however, is critically dependent on catalyst design, and a minute change of the structure of the catalyst may lead to a significant difference.

Catalytic systems shown in Table 1 are designed on the basis of the above-mentioned principle [25,26]. For the  $\text{M1}$  part, late transition metal species other than Ru are also employed (**6**, **7**, **9**). As the  $\text{M2}$  component, late transition metal species, in particular, group 10 (Pd, Pt; **1**, **2**, **3**) and group 9 (Co, Rh; **4**, **5**, **8**, **10**) species, are introduced, and the diiron species **11** is a mimic for the active site of hydrogenase [23]. Sakai and his coworkers have been investigating intramolecular catalysts containing a TB-like unit ( $\text{M1(PS)}$ ) and a square planar Pt unit ( $\text{M2(RC)}$ ) (**1**) [26], and reported that catalyst **1** produced  $\text{H}_2$  from water upon visible-light irradiation, though the TON was small. Subsequently, catalysts containing Pd-(**2**, **3**), Rh-(**4**), and Co- $\text{M2(RC)}$  units (**5**) were reported by Rau [27], Hammarström [28], Brewer [29], and Artero [30], respectively, and TON was improved to some extent. In the case of the **6**- $\text{RhCl}_3 \cdot 3\text{H}_2\text{O}$  mixing system reported by Nishibayashi, dinuclear species generated in situ has not been characterized satisfactorily [31]. At a glance at Table 1, however, TONs of the intermolecular systems (**II**) are superior to those of the intramolecular system (**I**) and, furthermore, the latter system turned out to be structure-sensitive. For example, an analogue of **1**, with the inverted BL arrangement,  $[(\text{bipy})_2\text{Ru}(\mu\text{-bipy-NH-C(=O)-phen})\text{PdCl}_2]^{2+}$ , showed no catalytic activity [26]; moreover, replacement of the bridging tpphz ligand in **2** by bipyrimidine resulted in complete loss of the catalytic activity [27].

Possible formal reaction mechanisms for the bimetallic catalysis are shown in Scheme 4. Two consecutive photosensitized electron transfer processes from  $\text{M1}$  to  $\text{M2}$  gives the hypothetical dianionic intermediate **J**. Two mechanisms are feasible for the final  $\text{H}_2$  production process, as readily anticipated from the knowledge of organometallic chemistry. Mono-protonation of **J** forms the monohydride intermediate **K**, further protonation of which at the M–H site generates  $\text{H}_2$  together with the starting catalyst **D**. On the other hand, di-protonation of **J** gives the dihydride intermediate **L**, which generates  $\text{H}_2$  and **D** via reductive elimination. Although discrimination of these mechanisms is difficult, it is concluded that, at least, for the cobaloxime systems (**5** and **10**) the former mechanism is operating [25d]. Very recently, Rau and his coworkers revealed the electron transfer pathway on **2**, i.e. from Ru to the



Scheme 4. Possible mechanisms for catalytic  $\text{H}_2$ -production by bimetallic species.

bridging tpphz ligand and then to Pd, by a combination of resonance Raman and ultrafast time-resolved absorption spectroscopy [32]. On the other hand, Hammarström observed deposition of Pd particles during photocatalysis by **3**, strongly suggesting that heterogeneous catalysis has a major contribution to the  $\text{H}_2$ -evolution [28]. Thus caution is needed in analyzing catalytic reaction mechanisms.

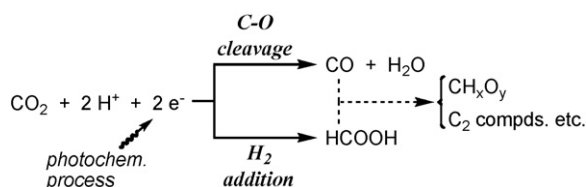
## 2.2. $\text{CO}_2$ reduction

Transformation of  $\text{CO}_2$  into useful chemical feedstocks is now regarded as one of solutions for the problem of the rise of  $\text{CO}_2$  concentration in the atmosphere, which may cause global warming. Because of the chemical inertness, only a few catalytic industrial processes using  $\text{CO}_2$  as a raw material have been developed [33]. However, fundamental research has provided potentially useful reactions of  $\text{CO}_2$ : electro- or photo-chemical reduction, transition metal catalyzed reaction with unsaturated hydrocarbons, and biomimetic fixation [34]. In particular, photochemical  $\text{CO}_2$  fixation is extremely important, because  $\text{CO}_2$  can be converted into useful chemicals by inexhaustible solar energy without sacrificing fossil fuel, as done by plants.

Studies of photochemical fixation of  $\text{CO}_2$  reported so far include reduction giving formic acid [35], acetic acid [36], malonic acid [37], formate [38], methane [39], and CO [40]. These examples can be divided into two types of reactions (Scheme 5); one accompanying C–O bond cleavage to give CO and the other resulting from  $\text{H}_2$  addition across the C=O bond. The former process is driven by formation of  $\text{H}_2\text{O}$ . While attempts to obtain organic compounds following the latter process have been made, there still remain problems to be overcome such as yield and selectivity. On the other hand, much improvement has been achieved for the CO formation.

$\text{CO}$  production from  $\text{CO}_2$  has been studied by using a variety of mononuclear catalysts such as  $\text{Re}(\text{bipy})$  complex and Co- and Ni-macrocycle complexes [41]. The pioneering work reported by Ziesel and Lehn on  $\text{Re}(\text{bipy})(\text{CO})_3\text{X}$  and following works revealed that rhenium complexes acted as photo- and electro-catalysts for reducing  $\text{CO}_2$  to CO [38a,b,42].

The mechanism of  $\text{CO}_2$  reduction by mononuclear Re species,  $[\text{Re}(\text{bipy})(\text{CO})_3(\text{X})]$  **12** ( $\text{X} = \text{SCN}$  (**a**),  $\text{Cl}$  (**b**),  $\text{CN}$  (**c**)), was revisited by Ishitani and his coworkers, and it has been proposed that the Re



Scheme 5. Two types of  $\text{CO}_2$  reduction.



**Table 1**  
Representative examples of photocatalytic H<sub>2</sub>-evolution from H<sup>+</sup> promoted by bimetallic systems.

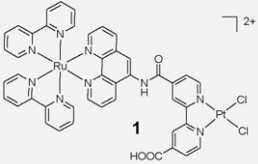
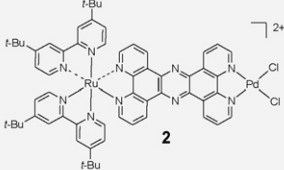
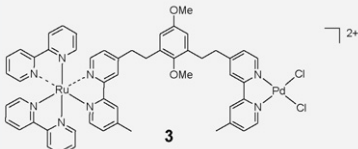
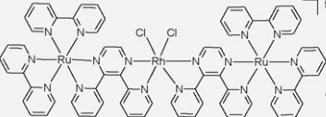
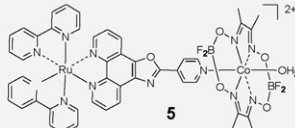
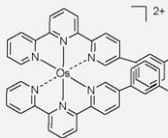
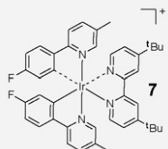
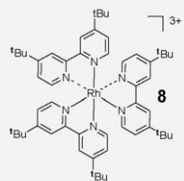
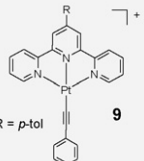
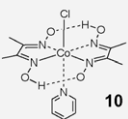
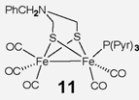
Solvent (donor: <i>D</i> )	M1(PS)	M2(PC)	TON <sup>a</sup> (Reaction time) [Reference]
<b>I-Type catalyst systems</b>			
H <sub>2</sub> O (EDTA) <sup>b</sup>			4.8 (10 h) [26a]
MeCN (NEt <sub>3</sub> )			56 (29 h) [27]
MeCN (NEt <sub>3</sub> )			30 (6 h) [28]
MeCN/H <sub>2</sub> O (DMA) <sup>d</sup>			30 (4 h) [29b]
Acetone (NEt <sub>3</sub> )			103 (15 h) [30]
MeCN/H <sub>2</sub> O (sodium ascorbate)		RhCl <sub>3</sub> ·3H <sub>2</sub> O	87 (18 h) 594 (240 h) [31]
<b>II-Type catalyst systems</b>			
H <sub>2</sub> O (TEOA) <sup>c</sup>	[Ru(bipy) <sub>3</sub> ] <sup>2+</sup> (TB)	[Rh(bipy) <sub>3</sub> ] <sup>3+</sup>	77 (6 h) [20b]
THF/H <sub>2</sub> O (TEOA)			5000 (22 h) [25b]
MeCN/H <sub>2</sub> O (3:2) (TEOA) <sup>c</sup>			~1000 (10 h) [25d]

Table 1 (Continued)

Solvent (donor: D)	M1(PS)	M2(PC)	TON <sup>a</sup> (Reaction time) [Reference]
MeCN/H <sub>2</sub> O(1:1) (ascorbic acid)	[Ru(bipy) <sub>3</sub> ] <sup>2+</sup> (TB)		4.3 based on <b>11</b> 86 based on TB (12 h) [25g]

<sup>a</sup> Turn-over numbers.<sup>b</sup> Ethylenediaminetetraacetic acid, (HOOC)<sub>2</sub>NCH<sub>2</sub>CH<sub>2</sub>N(COOH)<sub>2</sub>.<sup>c</sup> Triethanolamine, N(CH<sub>2</sub>CH<sub>2</sub>OH)<sub>3</sub>.<sup>d</sup> *N,N*-Dimethylaniline.

catalyst works in two ways. The present system is now regarded as a **II-A**-type catalyst system [43].

A mechanism proposed for the reaction catalyzed by [Re(bipy)(CO)<sub>3</sub>(NCS)] **12a** is shown in Scheme 6. Photo-excitation followed by electron transfer from TEOA forms the one-electron reduced species (OER **M**), which can be detected by spectroscopic methods.

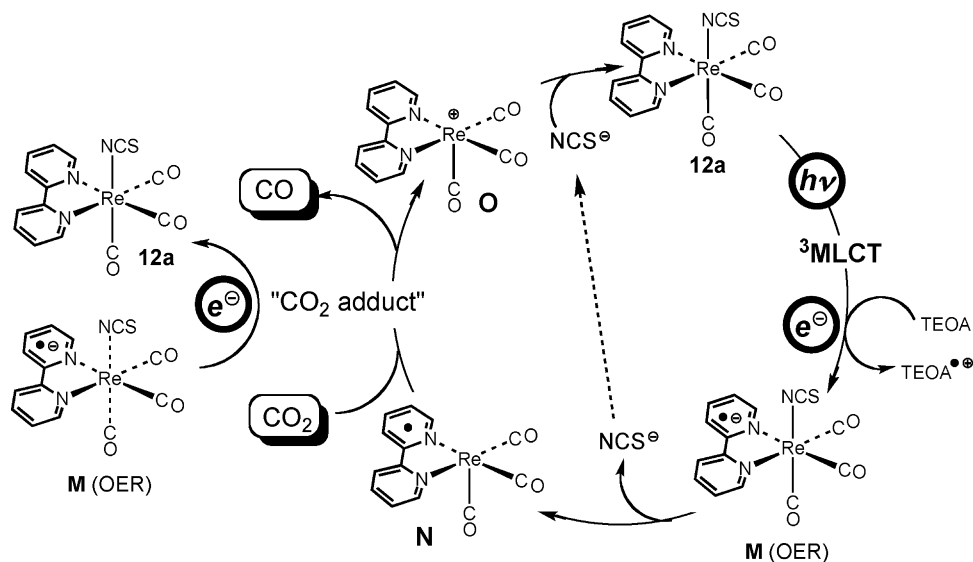
Subsequent dissociation of the NCS ligand gives the five-coordinate intermediate **N**, which captures a CO<sub>2</sub> molecule to form a “CO<sub>2</sub>-adduct”. For CO<sub>2</sub> reduction, two electrons are needed and the second electron is provided by another OER species (**M**). An overall 2e-reduction process on the Re center produces CO and the cationic intermediate **O**, which is trapped by the released NCS anion to regenerate **12**. Thus the Re catalyst works as the photosensitizing unit as well as the CO<sub>2</sub> binding site. In accord with this mechanism, substituent effects are noted. The Cl-derivative **12b** having short lifetime of OER shows lower catalytic performance, and the CN derivative **12c** which does not eliminate the CN ligand from OER, is totally inactive. Sharing the two roles of **12** by a 1:25 mixture of *fac*-[Re(bipy)(CO)<sub>3</sub>(CH<sub>3</sub>CN)]<sup>+</sup> (CO<sub>2</sub>-binding site) and [Re{4,4'-(MeO)<sub>2</sub>bipy}(CO)<sub>3</sub>{P(OEt)<sub>3</sub>}]<sup>+</sup> (photosensitizer) causes a significant increase of the quantum yield for CO formation from 0.30 to 0.59. While μ-CO<sub>2</sub> intermediate, [Re-C(=O)-O-Re], and hydroxycarbonyl intermediate, [Re-COOH], have been proposed for the “CO<sub>2</sub> adduct”, this important issue is still controversial and has remained to be clarified.

Studies on bimetallic catalyst systems combined with TB followed those on mononuclear systems. For example, Kimura

reported **I**- and **II**-type Ni-cyclam catalysts (Fig. 1) [44]. Visible-light irradiation of these complexes dissolved in aqueous ascorbate buffer solutions caused formation of a mixture of CO and H<sub>2</sub>. The catalytic activity was improved by catalyst design in the order shown in Fig. 1. The intramolecular catalysts (**I**; **14–16**) turned out to be better than the intermolecular system (**II**; TB/**13**). The catalytic activity, however, was inferior to, for example, the Re systems described below. The amount of CO formed by the most active catalyst was less than a stoichiometric amount, while catalytic turnover (TON ~5) was observed for H<sub>2</sub> production.

Recently, Ishitani succeeded in improving the catalytic activity by combining the Re functional group with TB [45]. The absorption ranges of the resultant **I-A**-type bimetallic catalysts were extended to the visible region so as to collect visible-light energy in a more effective manner. In addition, electron transfer from Ru to Re improved the efficiency of H<sub>2</sub>-production. A series of supramolecular Ru-Re complexes with different Re/Ru ratios was synthesized and their catalytic activities toward photoreduction of CO<sub>2</sub> to CO were studied systematically (Fig. 2). Complexes **17/18**, **19/20**, and **21/22** contain (CH<sub>2</sub>)<sub>2</sub>CHOH, (CH<sub>2</sub>)<sub>3</sub>COH, and diazole linkers, respectively. Irradiation of TEOA/DMF solutions containing the catalyst and BNAH (1-benzyl-1,4-dihydronicotinamide; a sacrificial electron donor) gave CO as the dominant product together with a small amount of H<sub>2</sub>. No HCOOH was detected. In this case, TEOA was not sufficient as an electron donor and, therefore, use of BNAH was essential.

Several interesting features were noted. (1) The best catalytic performance was observed for the Ru-Re<sub>3</sub> tetranuclear complex

Scheme 6. A mechanism proposed for CO<sub>2</sub> reduction catalyzed by [Re(bipy)(CO)<sub>3</sub>(NCS)] **12a**.

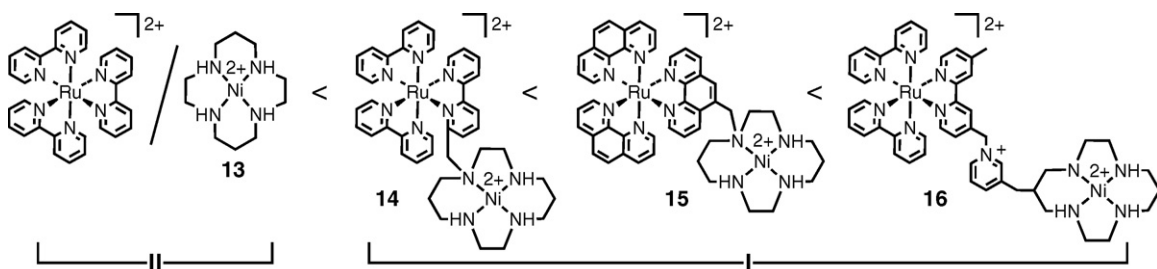


Fig. 1. Inter- and intra-molecular TB/Ni(cyclam) dyads.

**18**, although a mixture of mononuclear components showed catalytic activity to some extent [46]. A catalyst of a higher Re/Ru ratio (e.g. **18**) exhibited higher catalytic activity, whereas the activity per Re unit is not affected so much. (2) A remarkable substituent effect of the bipy ligands attached to Ru was observed for the **17**-type complexes. A catalyst with electron-donating bipy ligands (**17b**) turned out to show higher catalytic activity presumably because of the higher reducing ability of the Ru part. (3) One electron reduced species (OER) were detected for **19** by time-resolved transient absorption spectroscopy, and the added electron resided on the Ru-bound bipy end of the bridging ligands. Electron localization on the bridging ligand was suggested as another decisive factor. (4) In OER, electron transfer from the Ru side to the Re side on the bridging ligand finally led to reduction of CO<sub>2</sub> at the Re center. (5) Architecture of the bridging ligand is a key factor for the catalysis, as can be seen from comparison between **21** and **22**, where the arrangement of the metal fragments are switched.

### 2.3. Pd-catalyzed Sonogashira coupling reaction

In contrast to catalytic conversion of small inorganic molecules described above, little attention has been paid to catalytic organic transformation. Recently, Osawa, in collaboration with us, demonstrated an example of visible-light promoted catalytic C–C bond formation reaction, Sonogashira coupling reaction [47,48].

When a DMF-NEt<sub>3</sub> solution of aryl bromide **23** and 1-alkyne **24** was irradiated with visible light (>420 nm) in the presence of a **II-A**-type catalyst system composed of PdCl<sub>2</sub>(NCMe)<sub>2</sub> (6 mol%), P(*t*-Bu)<sub>3</sub> (6 mol%), and TB·(PF<sub>6</sub>)<sub>2</sub> (8 mol%), Sonogashira coupling proceeded to afford the coupling products **25** in excellent yields (Scheme 7). Addition of TB and visible-light irradiation were essential for the catalysis, whereas a Cu(I) salt usually added as a cocatalyst of thermal reactions to alkynylate the Pd intermediate [48] was not needed. Although the reaction was sluggish in the dark, irradiation caused significant acceleration of the reaction. When the light source was turned off, the coupling reaction stopped, and restarted

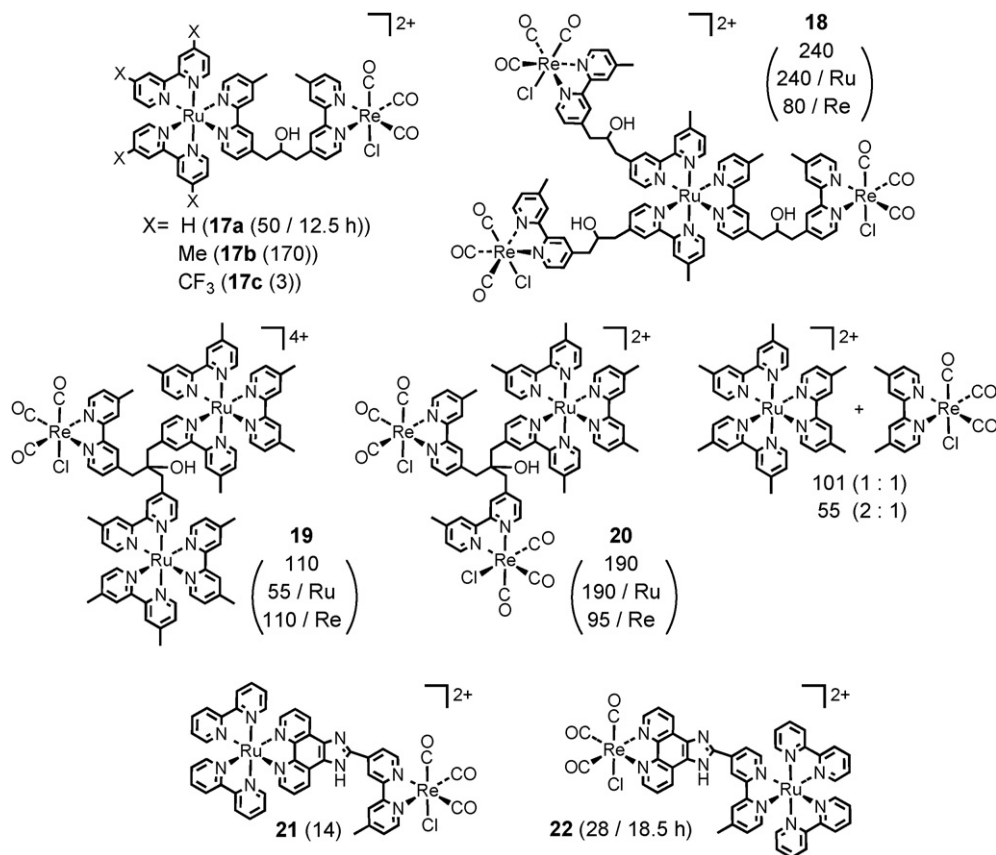
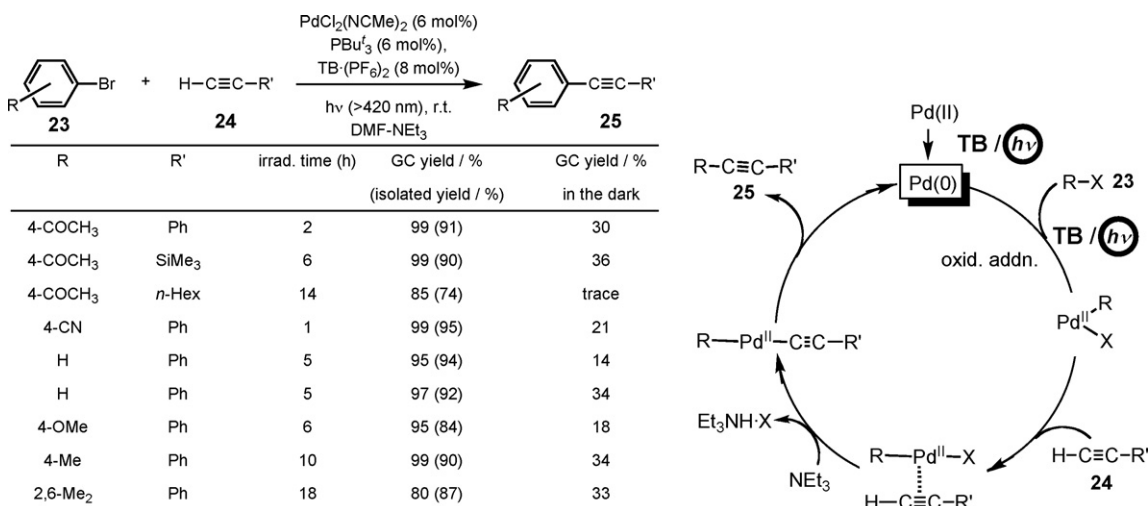


Fig. 2. Photocatalytic CO<sub>2</sub> reduction giving CO mediated by Ru–Re complexes. Numbers in parentheses are turnover numbers for production of CO. Irradiation time is 16 h unless otherwise stated.



**Scheme 7.** Photo-activation of Pd-catalyzed Sonogashira coupling reaction.

upon re-irradiation. Aryl bromides bearing electron-withdrawing substituents showed higher activity as observed for normal Sonogashira coupling under thermal conditions, while alkyl-substituted 1-alkyne was less reactive.

The catalytic activity can be tuned by the TB component (Scheme 8). While coupling of a less reactive aryl chloride such as *p*-chloroacetophenone **26** was catalyzed by the TB-containing catalyst system (34% yield), use of the derivative with electron-releasing *t*-Bu groups (**27**) improved the yield up to 47%. The nitro derivative **28** was less effective (10%). The apparent correlation with the reduction potentials of the TB components indicates that photo-excitation and electron transfer from the TB(I) species plays key roles in the catalysis.

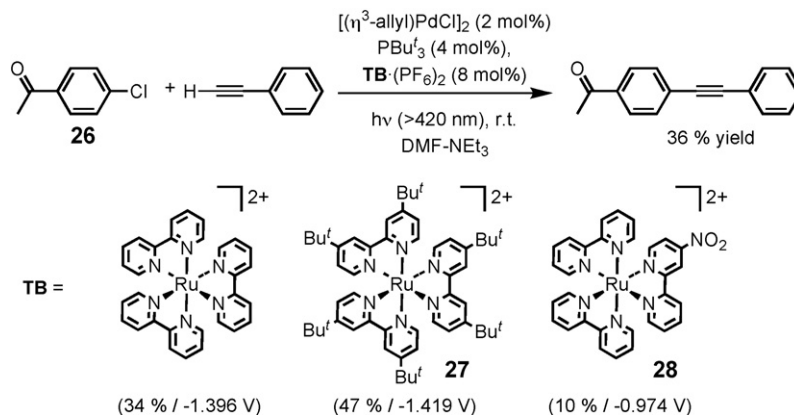
A couple of **I**-type catalysts coordinated by ligands bearing a TB-like substituent (e.g. **Pru**; for the structure, see Section 3.1) were also examined. Although, for example, PdCl<sub>2</sub>(**Pru**)<sub>2</sub> turned out to be catalytically active for photochemical Sonogashira reaction, the activity (Ph-Br + H-C≡C-Ph: 50% yield/2 mol% cat./24 h irrad.) was inferior to the intermolecular system **II** described above.

For the reactions shown in Scheme 7, addition of NEt<sub>3</sub> was essential, and the deterioration products of [NEt<sub>3</sub>]<sup>+</sup> (HNEt<sub>2</sub> and CH<sub>3</sub>CHO) resulting from electron transfer to TB\* were detected by GC-MS analysis, indicating that this system falls in the category of **II-A**. Because, however, (1) the catalytic reaction stopped upon turning off the visible-light source and (2) the oxidative addition ability was improved by the photocatalysis, energy transfer (**B**) from TB\* to Pd(II) also contributes acceleration of the catalytic

reaction. Although the net reaction does not require assistance by a reducing agent, it is suggested that TB-photocatalysis may promote the steps of (1) formation of a low valent Pd(0) species from a Pd(II) precursor and (2) oxidative addition of Ar-X (Scheme 7). We also found that photocatalytic Suzuki–Miyaura coupling and amination of haloarenes were also promoted by **II-A**-type catalyst systems [49].

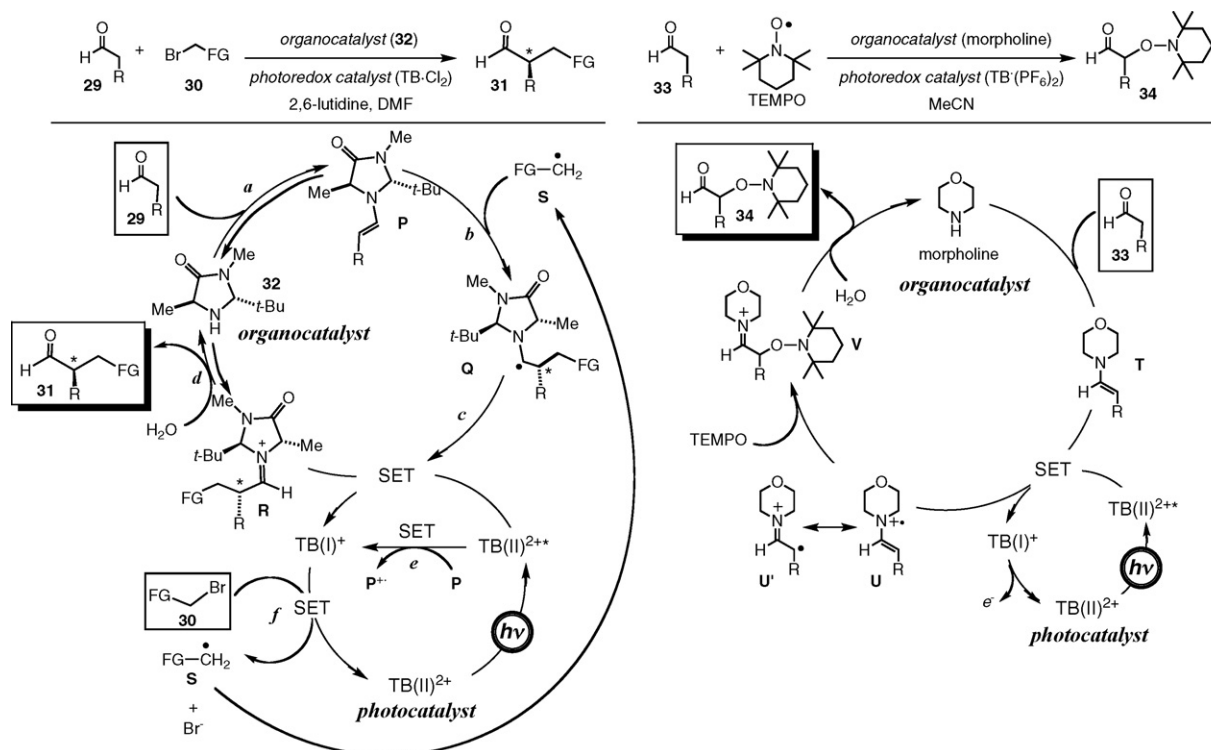
Before closing this section, let us briefly describe unique examples of oxidative photocatalysis by TB\* applied to organic coupling reactions (Scheme 9) [50,51], although they are catalyzed by mononuclear TB species. In the transformations described above, the sacrificial electron donor works as an electron donor but no attention has been paid to the resultant cation radical, which has a potential to be utilized as a reagent for organic synthesis and actually undergoes bond formation reactions as described below. Another feature of the following catalytic reactions is that the photocatalysis is combined with organocatalysis. Reductive transformations were also reported [52].

Recently, MacMillan reported asymmetric alkylation of aldehydes **29** with electron-deficient  $\alpha$ -bromocarbonyl compounds **30** mediated by a combined system of the photochemical TB catalyst and the chiral organocatalyst **32** (Scheme 9) [50]. The catalytic cycle is initiated by condensation of **29** and **32** giving the enamine intermediate **P** (step a), which serves as a sacrificial reducing reagent for TB(II)<sup>2+</sup> (step e). Single electron transfer (SET) from the resultant TB(I)<sup>+</sup> to **30** forms the radical intermediate **S** (step f), which couples with the enamine **P** to give the  $\alpha$ -aminoalkyl radical **Q** (step b). Oxidation (SET) of **Q** by TB(II)<sup>2+</sup> generates the iminium intermediate



**Scheme 8.** Substituent effect of the TB component.





Scheme 9. Catalytic systems combining photocatalysis and organocatalysis.

**R** (step c), hydrolysis of which affords the alkylated product **31** (step d).  $\text{TB(I)}^+$  formed by SET from **Q** (step c) causes generation of **S** from **30** (step f).

TB is responsible for (1) the initiation step, (2) generation of the radical intermediate, and (3) oxidation of the radical intermediate, all of which involve SET processes, whereas the organocatalyst **32** is responsible for (4) formation of the enamine intermediate **P**, (5) control of the stereochemistry of addition of **S** to **P**, and (6) stabilization of the resultant radical intermediate **Q** and oxidation thereof. The stereochemistry of the chiral center is determined at step b, and high enantioselectivities up to 99% is observed. The bulky *t*-Bu group shields the *Re* face of the enamine intermediate **P** to leave the *Si* face exposed for enantioselective radical addition.

Thus TB has a potential to serve as a versatile reagent for organic reactions involving SET processes. Recently, Koike et al. independently reported the photo-induced oxyamination of enamines and aldehydes **33** with TEMPO (Scheme 9) [51]. Here, too, SET from the enamine intermediate **T**, which is generated by condensation of aldehyde **30** with morpholine (organocatalyst), to the photochemically generated  $\text{TB(II)}^{2+}$  is involved as a key step. Coupling of the resultant radical intermediate **U/U'** with TEMPO forms the iminium intermediate **V**, which is converted to the oxyaminated product **34** via hydrolysis.

### 3. Catalytic reactions involving energy transfer (B-type transformations)

#### 3.1. Trans-to-cis isomerization of cyanostilbene

Compared to reductive transformations discussed above, catalytic reactions involving energy transfer are much less explored.

In 2001, Osawa et al. reported photocatalytic *trans*-to-*cis* isomerization of cyanostilbene (*trans*-**35**) (Scheme 10) [53] and, for this purpose, developed a very unique ligand **Pru**, in which a TB-

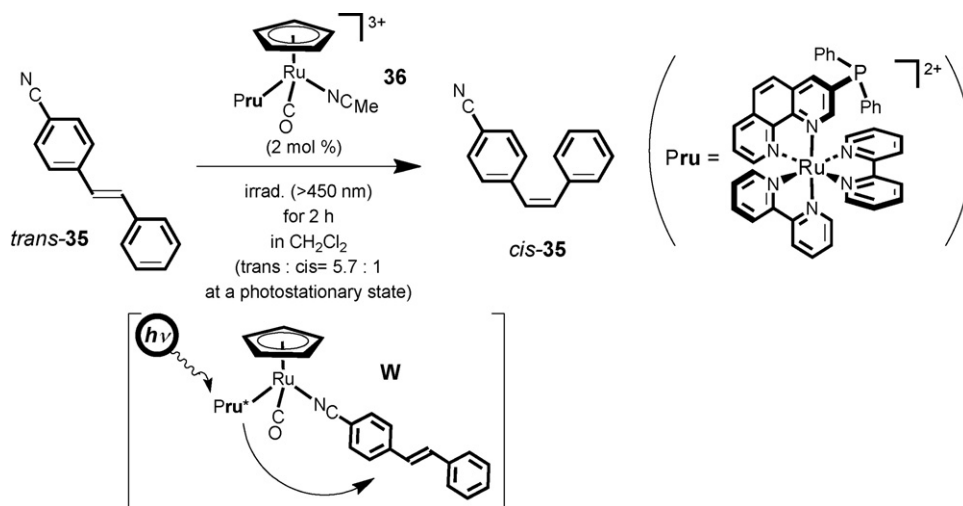
like photosensitizing  $\text{Ru}(\text{bipy})_2(\text{phen})$  fragment is combined with a tertiary phosphine ligand. It is expected that photoenergy adsorbed at the TB-like unit may be utilized at a reaction center nearby and, in this system, "coordination" is employed to assemble the reaction centers in proximity.

Two phenomena relevant to photosensitizing energy transfer were observed for the cationic  $\text{Ru}-\text{NCMe}$  complex **36**. While **36** was inert with respect to ligand substitution under thermal conditions, irradiation of visible light (>450 nm) caused substitution of the coordinated MeCN ligand by an externally added ligand such as  $\text{CD}_3\text{CN}$  and pyridine- $d_5$ . Because the related complex without the photosensitizing unit,  $[\text{CpRu}(\text{PPh}_3)(\text{CO})]^+$ , did not undergo ligand substitution even under irradiation, the ligand substitution on **36** is promoted by energy transfer from the TB-like unit to the CpRu center (**W**). The ligand substitution was not affected by  $\text{O}_2$  (an effective quencher of  $\text{TB}^*$ ), indicating that intramolecular energy transfer was very efficient. Furthermore, when a  $\text{CH}_2\text{Cl}_2$  solution of *trans*-**35** containing 2 mol% of the cationic  $\text{Ru}-\text{NCMe}$  complex **36** was irradiated, gradual catalytic isomerization to the *cis*-isomer (*cis*-**35**) was observed and reached a photoequilibrated state containing *trans*- and *cis*-**35** in a 5.7:1 ratio. Because the isomerization was retarded by addition of MeCN, it involves the substituted intermediate **W** and is promoted by efficient energy transfer from the TB-like unit to the coordinated **35**.

The present system is classified into **I-B**. Although a number of studies on energy transfer have appeared [54], to our knowledge, this is a rare example of a catalytic organic transformation induced by a photosensitizing metal species. In addition, the *trans*-to-*cis* isomerization is an up-hill reaction and, therefore, the light energy is stored as the form of the energetically less stable *cis*-isomer.

#### 3.2. Catalytic olefin dimerization promoted by $[(\text{bipy})_2\text{Ru}(\mu\text{-BL})\text{PdL}_n]$ species

It is remarkable that, as described in the previous section (Section 3.1), catalytic organic transformations can be promoted not



**Scheme 10.** Photochemical *trans*-to-*cis* isomerization of cyanostilbene **35** catalyzed by  $[\text{CpRu}(\text{Pru})(\text{CO})]^{3+}$  **36**.

only by electron transfer (**A**) but also by energy transfer (**B**) induced by photosensitization. We have been pursuing development of a new type of catalytic organic transformation, in particular, *catalytic C–C bond formation reaction*, taking into account the two possible mechanisms **A** and **B**.

We designed and prepared a series of bimetallic catalysts containing photosensitizing TB-like fragments as M1(PS),  $[(\text{bipy})_2\text{Ru}(\mu\text{-}\kappa_2\text{-}\kappa_2\text{-BL})\text{ML}_m]^{2+n}$  **37** (Fig. 3) and revealed that heterobimetallic Ru–Pd complexes showed catalytic activity toward olefin dimerization, which is the major topic to be discussed in this section.

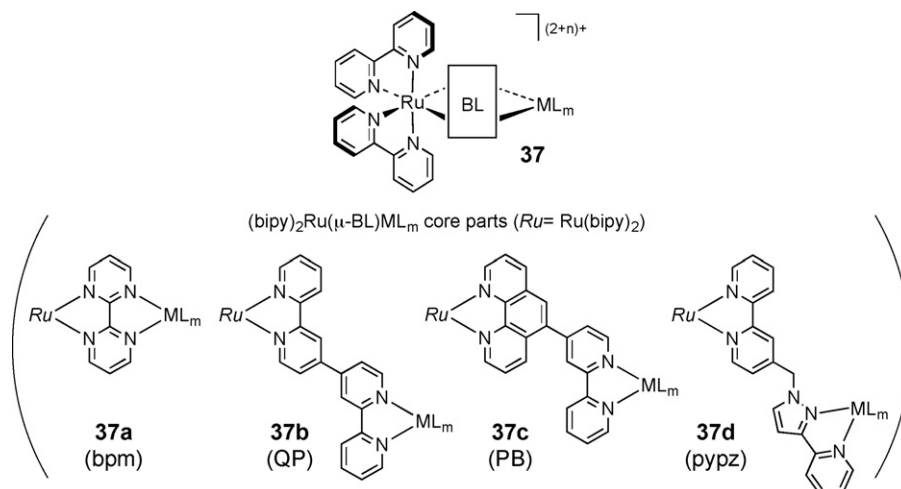
Bridging ligands (BL) used in our study are tetradentate ligands having two  $\kappa^2$ -coordination sites, one of which is of bipy-type for construction of the TB-like M1(PS) unit. Two types of BL are designed. In one type of BL such as bipyrimidine (bpm; **37a**), the four coordinating atoms are included in a rigid planar  $\pi$ -conjugated system. In the other type of BL such as quaterpyridine (QP; **37b**), phenanthrylbipyridine (PB; **37c**), and (pyridylpyrazolyl)bipyridine (pypz; **37d**), two bipy-like units are connected by a single bond or a methylene unit, which allows flexibility in arranging the two metal centers. For efficient electron/energy transfer, effective overlap of wave functions of the two components is crucial, and these two types of BL have advantages and disadvantages from this viewpoint. In the bpm complexes

**37a**, the two metal centers are directly connected by the planar  $\pi$ -conjugated ligand, in other words, the d-electron systems of M1 and M2 strongly interact with each other. If arrangement of the two metal centers is appropriate, the  $\pi$ -conjugation can lead to effective energy/electron transfer. However, if the ligand design is not appropriate, the rigid BL system cannot change its structure so as to fit an arrangement suitable for effective energy/electron transfer. In the other type complexes (**37b–d**), because the  $\pi$ -conjugated systems attached to the two metal centers are disconnected, electronic interaction between them is much weaker than that of the  $\mu$ -bpm complexes (**37a**). However, the more flexible linkers can lead to an arrangement of the two metal centers suitable for effective energy/electron transfer, though for an instant. Furthermore, compared to **II**-type catalyst systems, the two metal centers are located in close proximity and, therefore, we need not worry about the collision problem (Section 2.1).

In this section, discussion will be concentrated on heterobimetallic Ru–Pd catalysts, which show catalytic activity toward olefin dimerization.

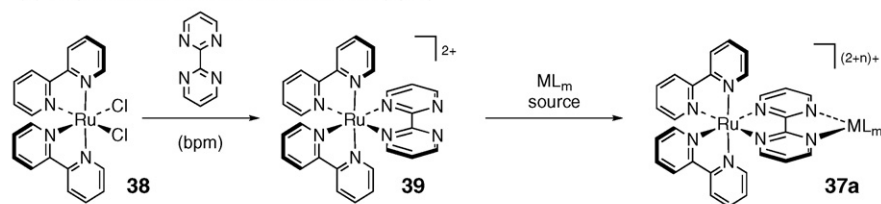
### 3.2.1. Synthesis of heterobimetallic catalysts

General synthetic routes to the bimetallic catalysts **37** are shown in Scheme 11.

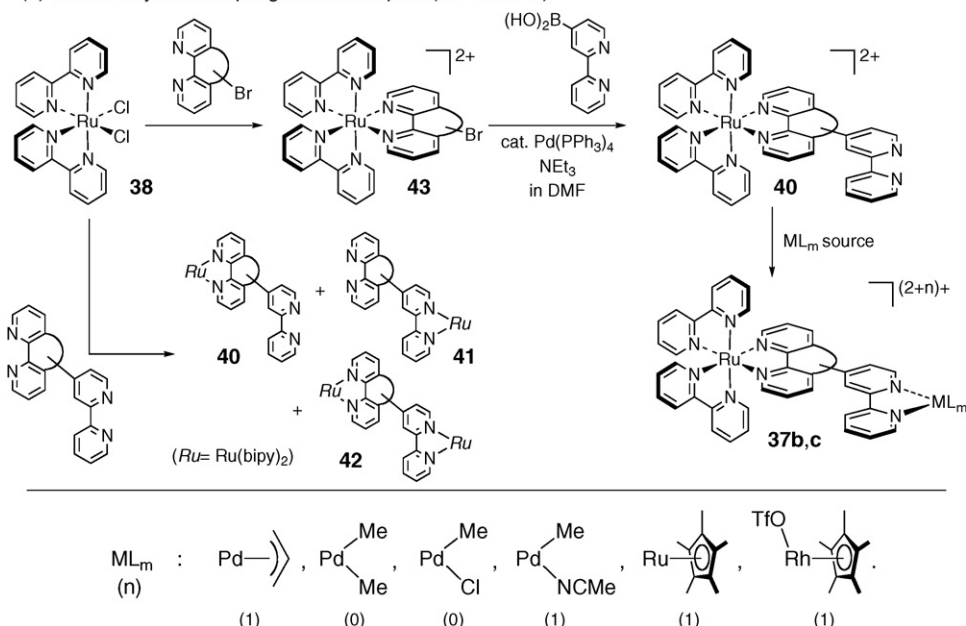


**Fig. 3.** Types of a series of bimetallic catalysts. ( $n$  is the charge of the  $\text{ML}_m$  part.)

## (a) stepwise introduction of BL and M2 (bpm)



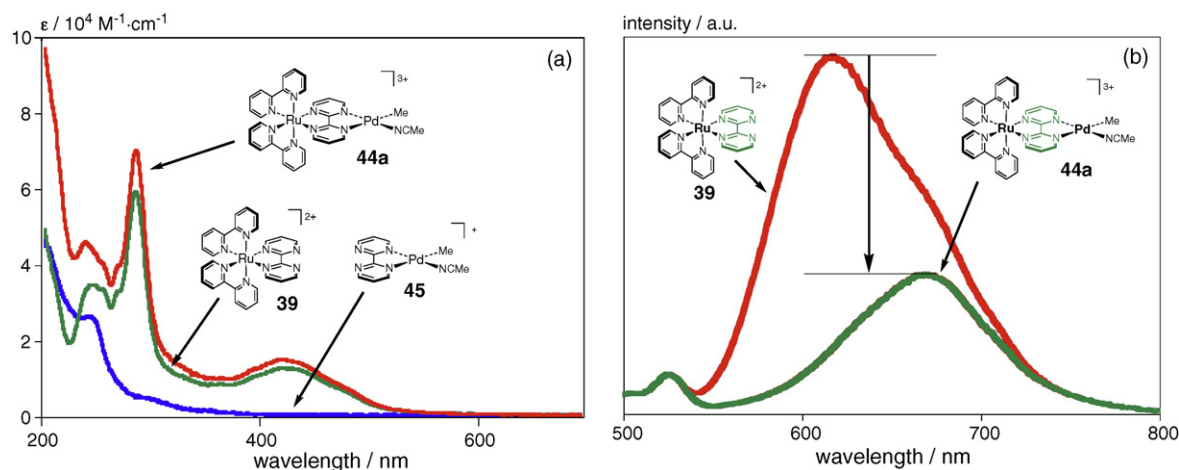
## (b) Suzuki-Miyaura coupling on Ru complex (QP and PB)

**Scheme 11.** Synthetic routes to the bimetallic catalysts **37**.

Synthesis of the  $\mu$ -bpm complexes **37a** is straightforward (*method a*) [17a,b,55]. Initial treatment of a labile Ru source,  $\text{Ru}(\text{bipy})_2\text{X}_2$  (**38**;  $\text{M1}(\text{PS})$ ), with BL (bpm) affords the mononuclear precursor having the free  $\kappa^2$ -coordination site,  $[(\text{bipy})_2\text{Ru}(\kappa^2\text{-BL})]^{2+}$  **39**. Subsequent treatment with a source of the second metal center ( $\text{M2}(\text{RC})$ ) furnishes the desired heterobimetallic catalysts,  $[(\text{bipy})_2\text{Ru}(\mu\text{-}\kappa^2\text{-BL})\text{ML}_m]^{2+n}$  **37a**. The first coordination of BL weakens the coordinating ability of the remaining  $\kappa^2$ -coordination site in **39** through the  $\pi$ -conjugation so as to provide the mononuclear adduct **39** in a selective manner rather than the homobimetallic adduct,  $[(\text{bipy})_2\text{Ru}(\mu\text{-}\kappa^2\text{-}\kappa^2\text{-BL})]^{4+}$ .

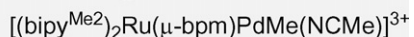
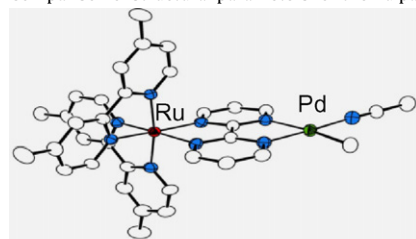
This is another advantage of  $\pi$ -conjugated ligands.

On the other hand, when the two  $\kappa^2$ -coordination sites in BL are electronically independent as in the case of **37b–d**, reaction analogous to *method a* affords a mixture of products containing the bimetallic adduct **42** and the undesirable 1:1 adduct **41** in addition to the desirable 1:1 adduct **40**, separation of which is tedious. In the case of **37b,c** this problem can be overcome by Suzuki–Miyaura coupling on the Br-substituted TB-derivatives **43** (*method b*) [17c]. Pd-catalyzed coupling with bipyrindylboronic acid in the presence of  $\text{NEt}_3$  furnishes the mononuclear precursors **40** with the free  $\kappa^2$ -

**Fig. 4.** Comparison of (a) UV and (b) emission spectra for  $[(\text{bipy})\text{Ru}(\mu\text{-bpm})\text{PdMe}(\text{NCMe})](\text{BF}_4)_3$  **44a** with those of mononuclear complexes having partial structures, **39** and **45**.

**Table 2**

Comparison of structural parameters for the Ru part (M1).



Complexes	bpm series ( <b>39</b> and <b>37a</b> )	QP series ( <b>37c</b> )	$[\text{Ru}(\text{bipy})_3]^{2+}$ (TB)
Ru–N (in Å)	2.041–2.093 (av. 2.069)	1.958–2.089 (av. 2.066)	2.041–2.066 (av. 2.056)
<N–Ru–N (in deg)	78.2–79.1 (av. 78.6)	78.4–79.6 (av. 78.9)	78.6–79.1 (av. 78.8)

coordination site, which are readily converted to the bimetallic catalysts **37b,c** upon treatment with sources for M2(RC). The pypz complexes **37d** are also prepared via *method b*; nucleophilic substitution of  $[(\text{bipy})_2\text{Ru}(\text{bipy-CH}_2\text{Br})]^{2+}$  by sodium pyrazolate provides the mononuclear precursor,  $[(\text{bipy})_2\text{Ru}(\kappa^2\text{-bipy-pypz})]^{2+}$  [**17d**].

A variety of metal fragments can be introduced to the M2 site, as we showed examples containing Pd, Ru, and Rh fragments. Above all, the cationic Pd species,  $[(\text{bipy})_2\text{Ru}(\mu\text{-bpm})\text{PdMe}(\text{NCMe})]^{3+}$  **44a**, turned out to be effective for olefin oligomerization as described below. Because of the polycationic nature of the obtained dinuclear complexes they are sparingly soluble in less polar organic solvents and their reactions were examined in nitromethane.

Thus we have established convergent synthetic methods for a series of bimetallic catalysts, in which various M1(PS), BL and M2(RC) fragments are coupled in a combinatorial manner. As a result, substituent effects on the three components can be investigated in detail in a systematic manner; in other words, the catalytic features of the bimetallic species can be finely tuned by introduction of appropriate substituents onto the three components. Catalytic properties of the  $\mu\text{-bpm-}$  (**37a**) and  $\mu\text{-QP-Pd}$  complexes (**37b**) will be discussed in detail in a latter section.

### 3.2.2. Spectroscopic and structural characterization of the bimetallic catalysts

**3.2.2.1. Spectroscopic characterization.** Formation of the heterobimetallic catalysts **37** is readily confirmed by spectroscopic analyses, which reveal that their spectroscopic data can be analyzed as a superposition of those of the components, M1, BL and M2, as typically exemplified by UV spectra (for **44a**, see Section 3.2.2.3 and Fig. 4a) and NMR spectra. For example, a  $^1\text{H}$  NMR spectrum (not shown) contains signals for each component with the intensities consistent with a 1:1:1 combination. These results indicate that, in the ground state, interaction between the two metal centers is not so strong as to perturb the basic properties of each metal component.

Electrochemical measurements provide useful information for properties of the reduced species resulting from photosensitization. Previous electrochemical studies of TB revealed appearance of a couple of reduction processes mainly localized on the bipy moieties in addition to the Ru(II)/Ru(III) oxidation process. Similar features are noted for the bimetallic catalysts **37**, although anodic shifts of the redox processes are caused by the attachment of M2. In some cases, redox waves for M2 appear. The redox potentials of the reduction processes are key features from the viewpoint of the reductive transformations, because redox potentials of such reduction processes are measures for the MO energy levels of the photo-excited state of M1(PS) (donor) and M2(RC) (acceptor) (Scheme 3). If the reduction process of the M2 part occurs in a more positive side compared to that of the M1 part,

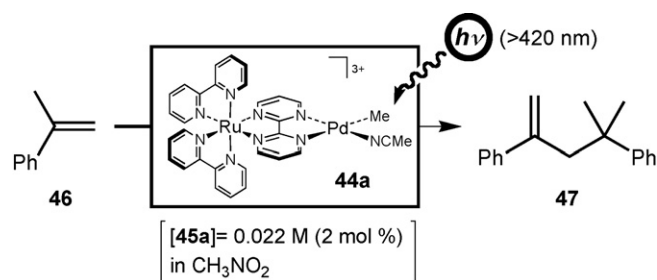
the excited electron at M1 can, in principle, be transferred to M2 in an exothermic manner (**F** → **G**; Scheme 3) or cause excitation at M2 (**E/F** → **I**). For **44a**, a series of ligand-centered reduction processes is observed at  $-0.85$ ,  $-1.54$ ,  $-1.85$ , and  $-2.16$  V (vs.  $\text{Fc}/\text{Fc}^+$ ); the former two processes are  $\mu\text{-bpm}$ -based, while the others are bipy-based. Although no Pd-centered redox process can be detected for **44**, comparison with related N-coordinated Pd(II) species (e.g. *cis*- $\text{PdCl}_2\{\text{bis}(1\text{-methylimidazol-2-yl})\text{glyoxal}\}$ :  $-0.74$  V) [57] indicates that Pd(II) species can be reduced by the 1e-reduced **44a**.

**3.2.2.2. Structural characterization.** Many of the mononuclear TB-like precursors (**39** and **40**) and the bimetallic catalysts **37** prepared in our laboratory were structurally characterized by X-ray crystallography. Structural features of the M1–BL and BL–M2 parts are similar to those of TB and a mononuclear counterpart corresponding to the M2 part, respectively, in a manner similar to the spectroscopic observation described above. For the bpm (**39** and **37a**) and QP complexes (**37b**), for example, the Ru–N distances and the N–Ru–N bite angles for the Ru parts are in very narrow ranges (distances  $<0.15$  Å; angles  $<1.2^\circ$ ) and are essentially the same as those of TB as compared in Table 2. The  $\mu\text{-bpm}$  ligands are so flat as to allow effective  $\pi$ -interaction between the two metal centers. In the case of **37c**, the dihedral angles defined by the phenanthroline and bipyridine planes are  $54.7^\circ$  ( $[(\text{bipy}^{\text{Me}_2})_2\text{Ru}(\text{PB})](\text{PF}_6)_2$ ) and  $61.5^\circ$  ( $[(\text{bipy})_2\text{Ru}(\mu\text{-PB})\text{Pd}(\eta^3\text{-allyl})](\text{PF}_6)_3$ ), indicating that the two bipy-like rings are not  $\pi$ -conjugated as in the case of the  $\mu\text{-bpm}$  complexes.

**3.2.2.3. Photophysical properties.** Assessment of photophysical properties of the heterobimetallic catalysts is essential for consideration of effects of visible-light irradiation on the catalysis. In this case, too, ground state electronic structure can be analyzed as a superposition of those of the two mononuclear units, M1(PS) and M2(RC), as is obvious from the UV–vis spectrum of  $[(\text{bipy})_2\text{Ru}(\mu\text{-bpm})\text{PdMe}(\text{NCMe})](\text{BF}_4)_3$  **44a** shown as a typical example (Fig. 4a) [17a,b]. The spectrum for **44a** is virtually summation of those for the mononuclear counterparts **39** and **45**.

By contrast, the emission spectrum of **44a** shown in Fig. 4b is not a simple summation of those for the analogues for the two mononuclear components (Fig. 4b). (**45** does not show an emission in this region.) Intensity of the emission of the Ru part substantially falls upon introduction of the second metal center (M2(RC)), suggesting that some energy transfer occurs, hopefully, to M2(RC) as we expected. Furthermore, a mixture of the mononuclear Ru component **39** and the Pd component **45** shows an emission spectrum essentially the same as that of **39**, indicating that the two metal units must be in the same molecule for effective energy transfer.





**Scheme 12.** Photocatalytic dimerization of  $\alpha$ -methylstyrene **46** mediated by **44a**.

Related photophysical features including lifetime of the excited states will be discussed later.

### 3.2.3. Selective photocatalytic dimerization of $\alpha$ -methylstyrene promoted by $[(\text{bipy})_2\text{Ru}(\mu\text{-bpm})\text{PdMe}(\text{NCMe})]^{3+}$ **44a** under visible-light irradiation: catalytic reaction and mechanisms

The bimetallic catalysts **37** were subjected to reactions with various organic substrates, and it was found that the Ru–Pd complex **44** was catalytically active for olefin dimerization under irradiation [17a,b, 58]. Herein discussion will be focused on olefin dimerization of  $\alpha$ -methylstyrene **46**, which was found at an early stage of our study and has been referred to as a standard reaction in assessing catalytic activity including substituent effects.

Irradiation of a nitromethane solution of  $\alpha$ -methylstyrene **46** by a Xe lamp ( $>420 \text{ nm}$ ) in the presence of 2 mol% of a  $\mu$ -bpm complex,  $[(\text{bipy})_2\text{Ru}(\mu\text{-bpm})\text{PdMe}(\text{NCMe})](\text{BF}_4)_3$  **44a**, caused selective dimerization of **46** to afford 4-methyl-2,4-diphenylpent-1-ene **47**, a dimer of **46**, in  $>90\%$  yield together with small amounts of trimers (Scheme 12). Because no sacrificial reagent was required and no other deteriorated byproduct was detected, the present catalytic reaction is classified as an energy transfer reaction of type **I-B** (Scheme 2).

First of all, effect of irradiation was examined (Fig. 5). Traces in Fig. 5 show the formation of the dimer **47** as a function of irradiation time. In the presence of 2 mol% of **44a**, most of **46** was converted into **47** within several hours, while no reaction took place at all in the dark. When the irradiation was turned off, the catalytic activity was lost but, upon re-irradiation, the catalytic reaction restarted finally to reach complete conversion. In addition, neither the mononuclear Pd complex,  $[(\text{bipy})\text{PdMe}(\text{NCMe})]^+$  **48**, having a partial structure

corresponding to M2 nor a mixture of the mononuclear components, TB and **48**, showed any catalytic activity indicating that (1) this reaction is an intramolecular photosensitizing reaction (**I-B**) and (2) the bimetallic structure is essential for the catalysis. (The bipy derivative **48** was used instead of **45** because of its thermal instability.) This situation is in sharp contrast to the photochemical Sonogashira reaction described in Section 2.3.

Scheme 13 shows a proposed mechanism for the olefin dimerization, which is supported by stoichiometric reactions in  $\text{CD}_3\text{NO}_2$ , as described below. The initial event is insertion of the olefin **46** into the Pd–Me bond in **44a** (step a). Subsequent  $\beta$ -hydride elimination from the resultant alkyl intermediate **X** gives the active hydride intermediate **Y** (step b). The initial adduct **X** consisting of a pair of diastereomers (with the chiral centers at the Ru center and the  $\alpha$ -carbon atom of the 2-phenylbut-2-yl group) and the eliminated olefin, (*E*)-2-phenyl-2-butene **49**, were detected and characterized in situ by  $^1\text{H}$  NMR but the hydride intermediate **Y** was so reactive as to immediately undergo 2,1-insertion of **46** to form the phenyl-2-propyl intermediate **50** (step c), which was characterized by  $^1\text{H}$  and  $^{13}\text{C}$  NMR. Formation of **50** was also supported by isolation and structural characterization of the stable  $\eta^3$ -benzyl species **51** (an isomer of the  $\sigma$ -bonded form **50'**) derived from **44a** and styrene. Because reaction proceeded up to this stage (**50**) even in the dark, it is concluded that irradiation promotes subsequent 2,1-insertion of a second molecule of the olefin **46** to form **Z** (step d). Final  $\beta$ -hydride elimination from the methyl group produces the dimer **47** as well as the hydride intermediate **Y** (step e) to complete the catalytic cycle.  $\alpha$ -Methylstyrene dimer **47** is a useful chemical and used as lubricant and diluent. In contrast to the conventional acid-catalyzed dimerization reaction forming a mixture of isomers by way of carbocationic intermediates [59], the present photochemical method produces **47** as a single isomer. A combination of (1) the two consecutive specific 2,1-insertion of the olefin and (2) the specific  $\beta$ -hydride elimination from the methyl hydrogen atom (indicated by an arrow) leads to the excellent regiochemistry of the coupling (formation of the head-to-tail dimer **47**) and the double bond formation (terminal olefin product), respectively. The bulky substituents may hinder abstraction of the methylene hydrogen atoms in **Z** leading to another isomer **47'**.

### 3.2.4. Improvement of the catalytic performance

The photocatalytic dimerization of  $\alpha$ -methylstyrene **46** turned out to be highly selective but the catalytic activity had room

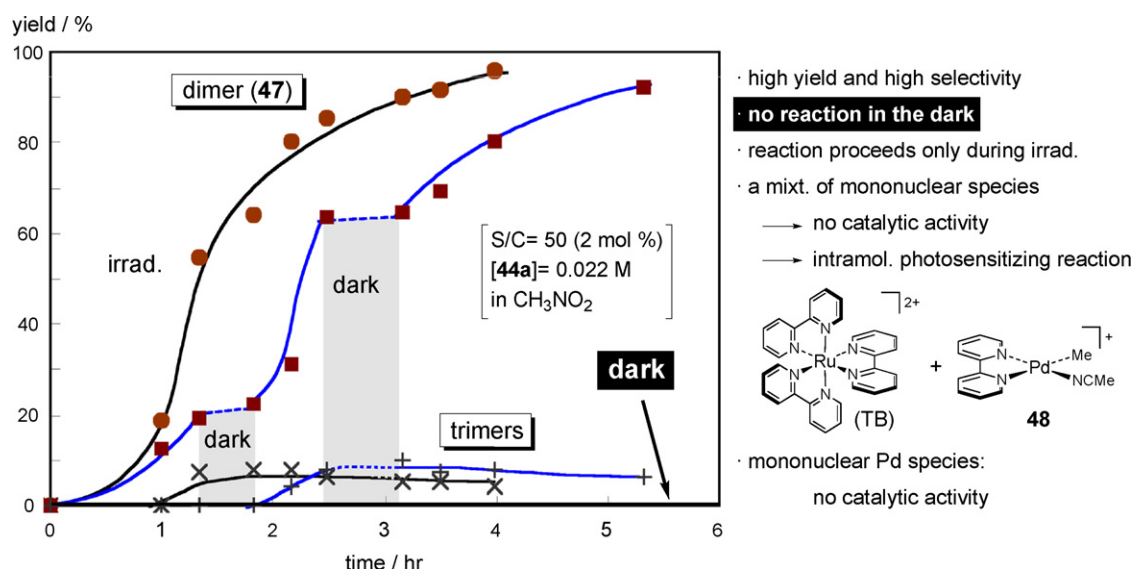
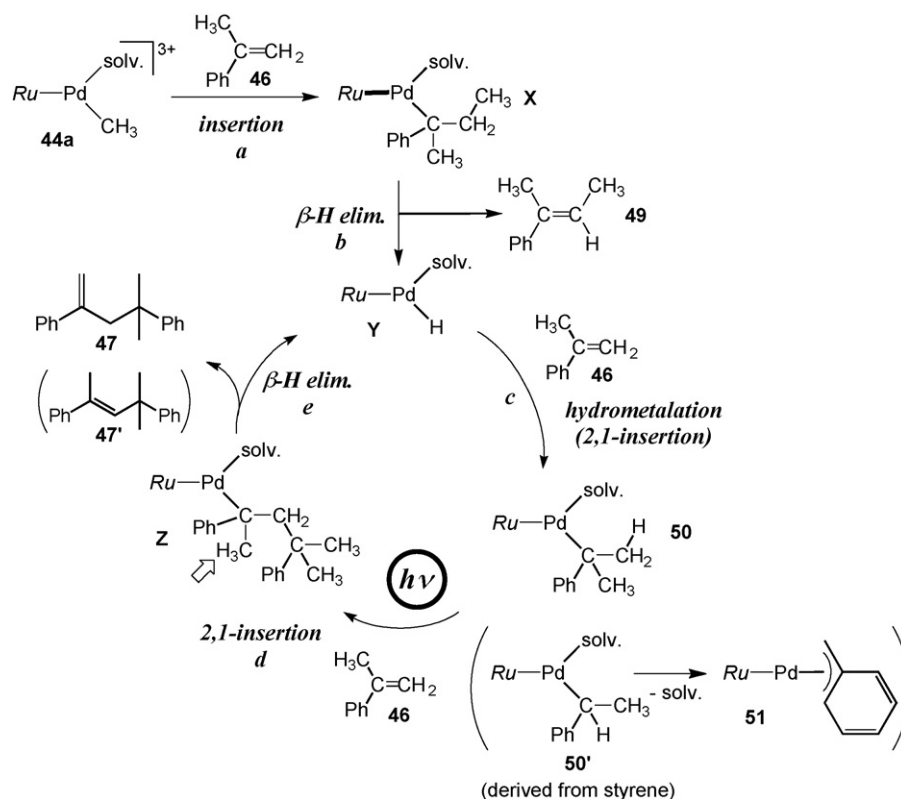


**Fig. 5.** Formation of **47** by photocatalytic dimerization of **46**.





**Scheme 13.** Catalytic cycle proposed for dimerization of **46**.

for improvement. Of many possible factors, which would affect the efficiency of the catalytic systems, we considered two factors: lifetime of the excited states and control of direction of energy/electron transfer (Table 3). As the lifetime of the excited state becomes longer, the chance of energy/electron transfer will increase. Furthermore, for efficient energy/electron transfer to M2, photochemical MLCT transition should occur from Ru to the direction of BL attached to M2 but not to the terminal bipy ligands, because the latter process simply goes back to the original state through deactivation (*path a'* or *b'* in Scheme 3), i.e. no net reaction.

In order to examine the first point, the QP complexes **52** were prepared (Table 3) [17c]. In **52**, the TB fragment is  $\sigma$ -bonded to the bipy part of the Pd fragment. The lifetimes of the triplet state of

the QP complexes **52** retaining the TB fragment would be longer than those of the bpm complexes **44** and comparable to that of TB but the symmetrical coordination structure around the Ru atom may not always result in effective energy/electron transfer to the Pd center (M2). On the other hand, while the lifetime of the excited state of the  $\mu$ -bpm catalyst **44** may be shorter, the unsymmetrical structure may lead to efficient energy/electron transfer to the Pd center.

**3.2.4.1. Lifetime elongation: comparison with the QP system.** Lifetimes of the excited states of the bpm and QP complexes are summarized in Scheme 14.

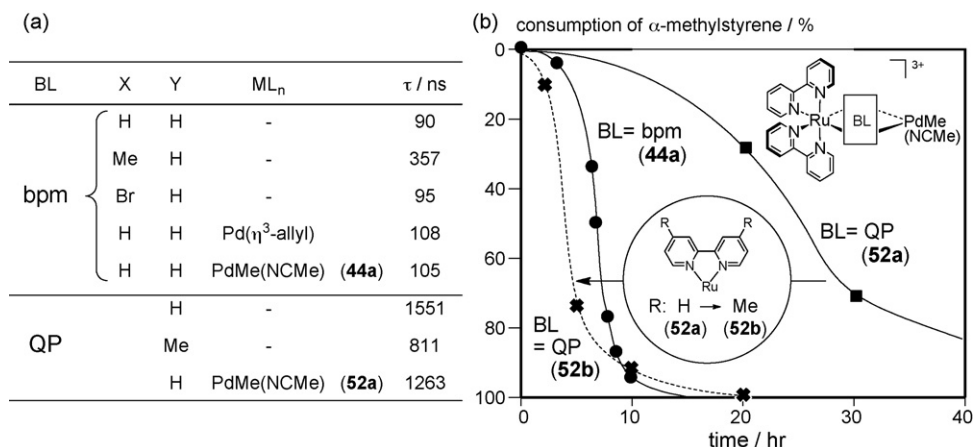
As can be seen from the table, the lifetimes of the excited states of the QP complexes including **52a** are comparable to or even longer than that of TB (1.1  $\mu$ s), whereas those of the bpm complexes including **44a** are much shorter: bpm (<400 ns) < QP ~ TB [56]. Thus, for keeping a longer lifetime of the excited state, retention of the TB-like partial structure is essential. But the catalytic activity was not apparently correlated with the lifetimes, as shown in Scheme 14b; the  $\mu$ -bpm complex **44a** showed catalytic activity much higher than that of the  $\mu$ -QP complex **52a**.

As will be discussed later, the catalytic activity can be tuned by introduction of appropriate substituents onto the terminal and bridging ligands and, in this case, attachment of methyl groups to the Ru(bipy)<sub>2</sub> part of the QP complex (**52b**) causes substantial improvement of the activity, even better than that of the original, unmodified bpm catalyst **44a**. These results indicate that the long lifetime of the excited state is not always an essential factor for the present catalytic olefin dimerization.

**3.2.4.2. Controlling direction of the energy/electron transfer and DFT analysis of substituent effects.** Taking into consideration the results described above, we next examined controlling direction of the

**Table 3**  
Possible factors affecting catalytic activity.

bpm		QP
<p><b>44</b></p> <p>(X: H, Me, CF<sub>3</sub>, NMe<sub>2</sub>) (Y: H, Me, Bu<sup>t</sup>, pyrenyl)</p>		<p><b>52a</b></p> <p>[Ru(bipy)<sub>3</sub>]<sup>2+</sup> unit</p>
Ru center with bipy-like ligands [(bipy) <sub>2</sub> + bpm]	structural features	Ru(bipy) <sub>3</sub> center $\sigma$ -bonded to the Pd unit
shorter life-time	life time of the excited state	long life-time comparable to Ru(bipy) <sub>3</sub>
anisotropic MLCT at Ru	direction of electron/energy transfer	isotropic MLCT at Ru



**Scheme 14.** (a) Lifetimes of complexes containing bpm and QP ligands and (b) catalytic activity of the bimetallic catalysts for **46**-dimerization. For the substituents X and Y, see the structure in Table 3.

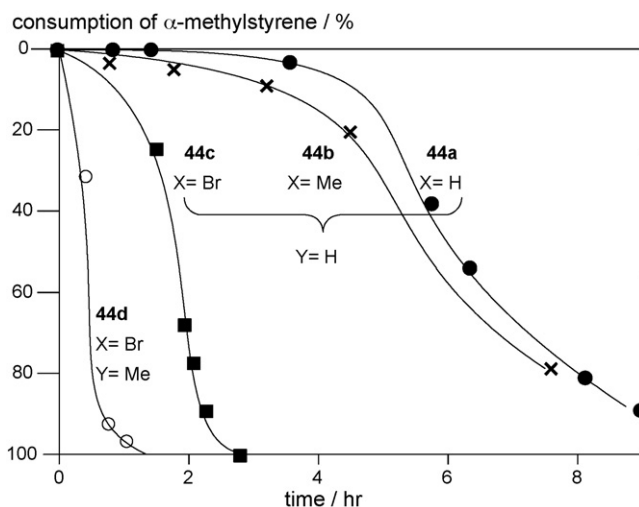


**Fig. 6.** Substituent effects on dimerization of **46** catalyzed by **44**.

energy transfer by introducing substituents to the bimetallic catalyst **44**.

Introduction of methyl groups to the μ-bpm ligand (X; cf. Table 3) (**44b**) did not affect the catalytic activity so much but that

of electron-withdrawing bromine atoms (**44c**) caused a significant enhancement of the catalytic activity (Fig. 6). Furthermore, introduction of electron-releasing methyl groups to the terminal bipy ligands (Y) (**44d**) enhanced the catalytic activity; 50 equivalents of **46** were converted into **47** within 1 h.

Then changes of the electron densities at the metal centers brought about by introduction of the substituents X and Y were investigated. Electron-densities at the Ru centers were affected by the substituents as judged by CV data (Fig. 7). As for the Pd parts, because Pd is rather featureless with respect to spectroscopic data, the electron densities were estimated by DFT. As can be seen from Fig. 7, electron densities (Mulliken population) at Pd are virtually the same irrespective of the substituents. Furthermore, when CO vibration frequencies of the rhodium carbonyl derivatives **53** are compared, again they are virtually the same, indicating that the substituents (X and Y) affect the electron densities at the Ru centers significantly but hardly affect those at the M2 centers (Pd, Rh). Thus, although we anticipated that the substituents would affect the electronic state of the Pd center, with which the substrate interacts, these results reveal that the substituent effects do not reach the Pd centers in the ground state. If so, what kind of factors is affected by the substituents?

In order to consider the substituent effects, DFT calculations were performed for four derivatives of **44** (Y = H, X = H (**44a**), Me (**44b**), Br (**44c**); Y = Me, X = Br (**44d**)), and Fig. 8 shows energy dia-

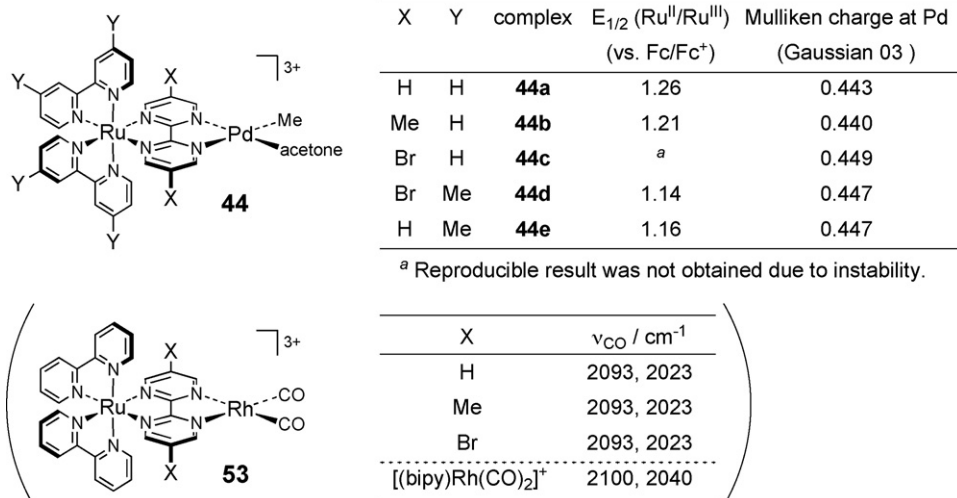


**Fig. 7.** Comparison of electron densities at Pd and Rh of the bpm complexes bearing various substituents.

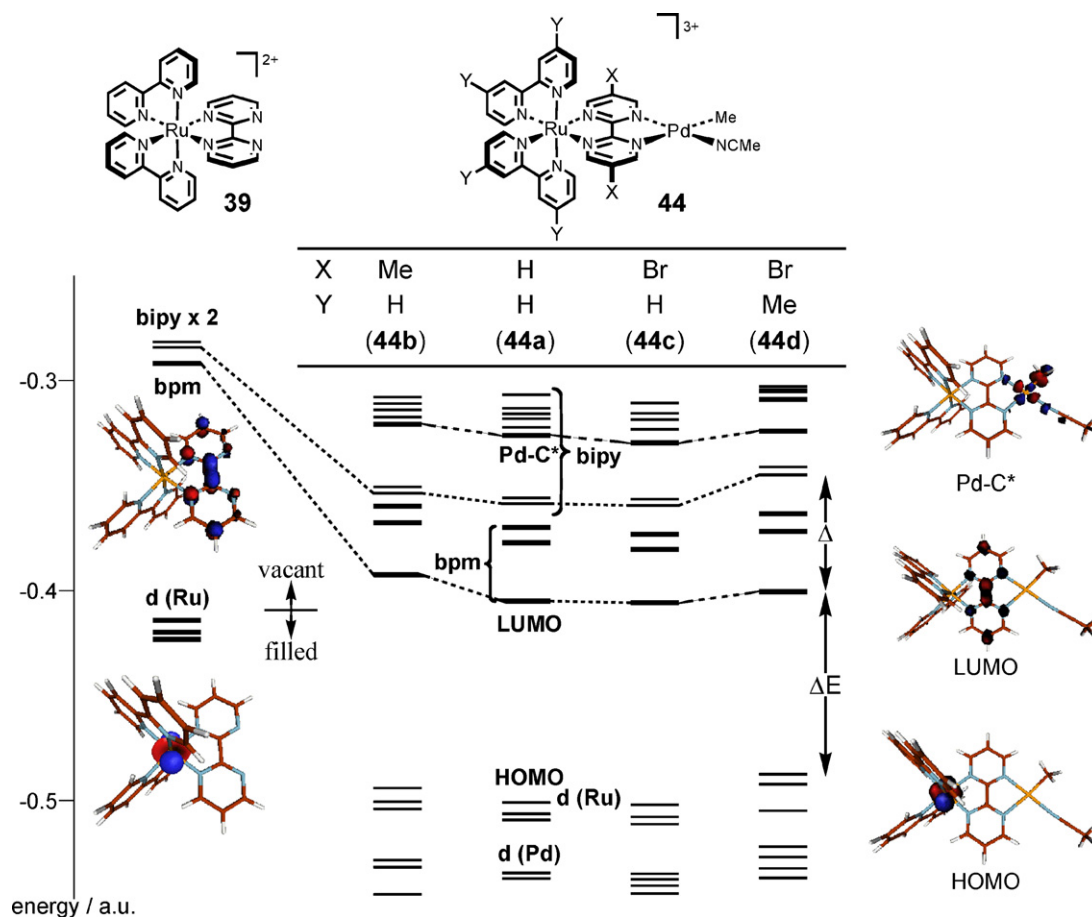
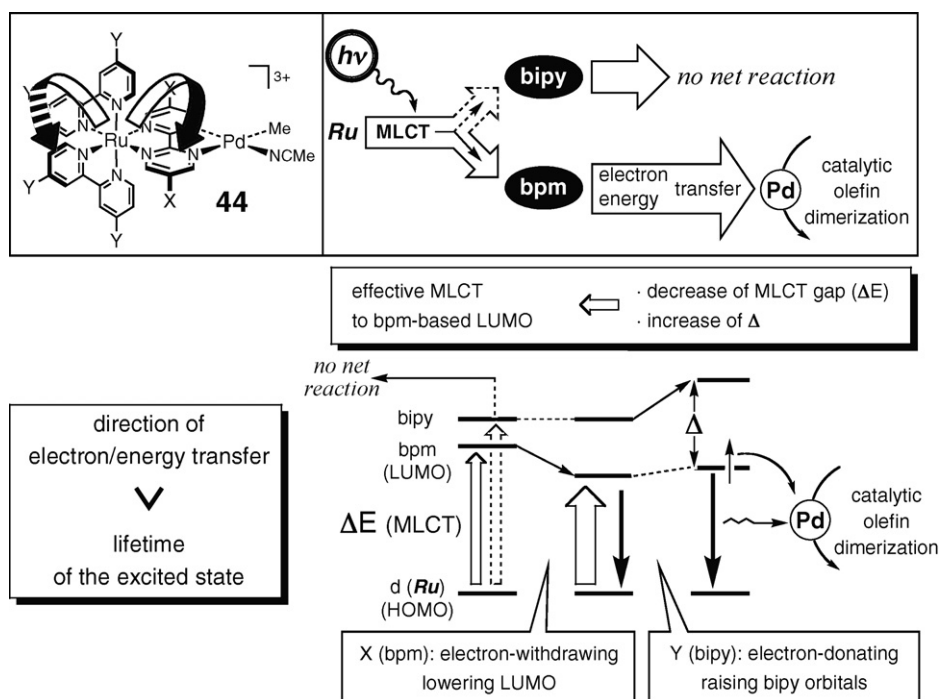


Fig. 8. Comparison of the energy levels of the frontier orbitals for substituted 44.



Scheme 15. Interpretation of the DFT results.

gram of their frontier orbitals obtained by DFT calculations [17b]. The HOMO and LUMO orbitals are mainly based on the d orbitals of the Ru atom and the  $\mu$ -bpm ligand orbitals, respectively. The vacant bipy ligand orbitals are located slightly higher in energy compared to the vacant bpm orbitals, and the Pd–C  $\sigma^*$  orbitals are laid further higher in energy. We consider that efficient MLCT from the occupied Ru orbitals to the vacant bpm orbital (LUMO) in preference to the vacant bipy orbital should promote catalysis at the M2 site, because MLCT to the terminal bipy ligands having no interaction with M2 simply results in deactivation leading to the original state, i.e. no net reaction (see also Scheme 15). There are two ways to promote preferential MLCT to bpm (BL). A large energy difference between the vacant bpm and bipy orbitals ( $\Delta$ ; Fig. 8) should result in preferential MLCT to  $\mu$ -bpm. Compared to mononuclear species **39**, attachment of the cationic Pd fragment causes significant lowering of the  $\mu$ -bpm-based orbitals including LUMO to increase  $\Delta$ . Furthermore, a smaller MLCT energy gap ( $\Delta E$ ) should promote MLCT itself. As the substituent X becomes electron-withdrawing as going from methyl (**44b**) to hydrogen (**44a**) and then bromine group (**44c**), energy levels of the LUMO orbitals are lowered, whereas the other orbitals are not affected so much. The lowering of the  $\mu$ -bpm-based LUMO level results in an increase of  $\Delta$  as well as a decrease of  $\Delta E$  to induce preferential MLCT transition to  $\mu$ -bpm.

How about the effects of the bipy substituents (Y)? Introduction of electron-releasing substituents onto bipy (Y) brings about rising of the vacant bipy orbital, while other frontier orbitals are not affected significantly. As a result,  $\Delta$  becomes larger so as to promote preferential MLCT to the  $\mu$ -bpm ligand.

The results of the DFT calculations are schematically presented in Scheme 15. Introduction of electron-withdrawing substituents onto the bpm ligand (X) causes lowering of the LUMO to increase  $\Delta$  and diminish the transition energy  $\Delta E$ . Introduction of electron-releasing substituents (Y) causes rising of the bipy orbitals to further increase  $\Delta$  and MLCT transition occurs to the bpm orbital in

a selective manner to promote the catalytic reaction. A combination of these two substituent effects causes the significant acceleration of the catalytic olefin dimerization.

These results lead to a conclusion that, in the present case, controlling the direction of the electron or energy transfer is a factor more crucial than the lifetime of the excited state.

As discussed in the previous section (Section 3.2.4.1), it is evident that the visible-light irradiation promotes insertion of the second equivalent of the substrate (**50**  $\rightarrow$  **Z** in Scheme 13). Although we have no experimental support at the moment, one of possible interpretations for the promotion effect is as follows. The first event should be replacement of the coordinated solvent molecule in **50** by the olefinic substrate. The most likely process following the substitution is the Ru-to- $\mu$ -bpm MLCT transition brought about by irradiation. The MLCT to  $\mu$ -bpm causes development of a negative charge on the  $\mu$ -bpm part (like **M** in Scheme 6), possible effects of which involve weakening of the Pd–Me bond brought about by electron transfer to its  $\sigma^*$  orbital and *trans*-influence labilizing the alkyl group to be transferred to the coordinated olefin [60]. Further study is needed to reveal the reaction mechanism.

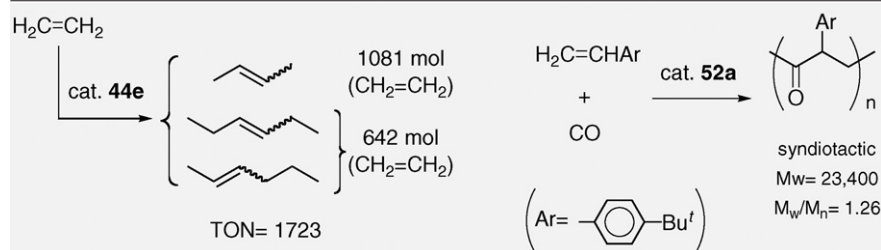
### 3.2.5. Photocatalytic olefin dimerization by **44**- and **52**-type catalysts

The modified catalysts were applied to other substrates (Table 4). Styrene and ethylene were also converted to the head-to-tail dimers and oligomers, respectively, in an efficient manner. Of the catalysts examined, the  $\text{bipy}^{\text{Me}_2}\text{-bpm}^{\text{Br}_2}$ -complex **44d** turned out to be most active. Ethylene was converted into a mixture of stereoisomers of 2-butenes and 2- and 3-hexenes, and the turnover number exceeded 1700 indicating that the less bulky substrate showed higher reactivity to undergo multiple insertion. By contrast, methyl acrylate gave isomeric mixtures of the head-to-head dimers, and the parent complex **44a** showed activity better

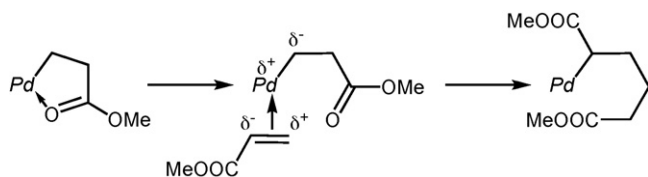
**Table 4**

Photocatalytic olefin dimerization (oligomerization) of olefins ([**44**] = 0.022 M/2 mol%, irradiation (>420 nm) for 8 h, in  $\text{CH}_3\text{NO}_2$ ).

Olefin	Dimer (Oligomer)	TON		
		Y = H		Y = Me
		X = H ( <b>44a</b> )	X = Br ( <b>44c</b> )	X = Br ( <b>44d</b> )
	$\text{C}_{2n}\text{H}_{4n}$ ( $n = 2, 3$ ; mixt. of isomers)	1400	1330	1723
		0.11	21	38
		12	>50	>50
		27	0	0







**Scheme 16.** A part of the proposed mechanism for insertion of methyl acrylate.

than the modified ones, **44c,d**, which were totally inactive. The QP catalyst **52a** (for structure, see Table 3) was not effective for the olefin dimerization but served as a catalyst for syndiotactic CO–styrene copolymerization to form the polyketone with the molecular weight over 23,000.

The different catalytic behavior observed for methyl acrylate can be interpreted as follows (Scheme 16). The initial part of the mechanism is similar to that of Scheme 13 but, when the electronic demands of the Pd–H part in **Y** are considered ( $\text{Pd-H}^+ \leftrightarrow \text{Pd} + \text{H}^+$ ), nucleophilic metal center attacks the terminal methylene carbon atom as in the case of Michael addition (1,2-insertion). In the resultant primary alkyl metallacyclic intermediate, the Pd–C part is polarized like  $\text{Pd}^{\delta+} \text{C}^{\delta-}$  so that the alkyl group attacks the terminal methylene carbon atom (2,1-insertion) to produce the head-to-head dimers after  $\beta$ -elimination. As for the catalytic activity, the electron-withdrawing bromine atoms in **44c,d** should increase Lewis acidity of the Pd center to stabilize the five-membered cyclic intermediate (Scheme 16) and hinder dissociation of the oxygen atom, which is essential for insertion of the second substrate.

#### 4. Future prospects

Increasing attention has been focused on utilization of solar energy as a chemical potential, and a substantial number of photocatalytic molecular transformations have been developed so far, as summarized in this review article. Not only electron transfer but also energy transfer can operate as a mechanism for a variety of photocatalytic transformations, which have been extended to many types of molecular transformations including organic ones. Photochemical processes are analyzed in detail by using modern equipments and techniques but still there are many problems to solve. First of all, reaction mechanisms, in particular, for organic transformations, have remained to be clarified. This is because (1) photochemically generated intermediates are usually so short-lived that it is hard to detect and characterize them and, in addition, (2) catalytic reactions consist of a series of complicated multi-step thermal and photochemical elementary processes, which are hard to be investigated separately.

A more difficult problem is catalyst design. We can easily categorize previously reported reactions according to the **I/II** and **A/B** classifications. But, at the moment, we cannot tell which catalyst system is suitable for a particular transformation. *You never know till you have tried.* This means that design of bimetallic photocatalysts is at an immature stage. For effective energy/electron transfer, controlling overlap of wave functions of catalyst components is essential but intra- and inter-molecular catalyst systems have advantages as well as disadvantages concerning this point, as discussed in Section 3.2. Because situations are different from case to case (e.g. catalytic reaction and catalyst), catalyst design has remained to be a tough problem to tackle.

One of advantages of photocatalytic systems is that they have the potential to conduct up-hill transformations, which cannot be realized by thermal reactions. By using metal photocatalysts, a couple of photochemical up-hill transformations such as  $\text{H}^+$ - and  $\text{CO}_2$ -reduction discussed in Sections 2.1 and 2.2, respectively, have been achieved. But still there is room for improvement of the activity and selectivity. Additionally, of organic transformations

discussed in this article, the *trans*-to-*cis* isomerization (Section 3.1) is the only example of up-hill transformation, and the others are down-hill reactions. If metal-sensitized photocatalytic reactions will have been developed to a satisfactory level in the future, many catalytic transformations can be conducted under very mild conditions in selective manners, like photosynthesis. Bimetallic photocatalysis, where required catalytic functions are shared by multiple metal catalyst components, will contribute to development of such unique catalytic chemical transformations.

Continued accumulation of reaction data and mechanism analysis will lead to development of practical bimetallic photocatalysts.

#### Acknowledgements

We gratefully acknowledge financial supports from the Japan Society for Promotion of Science and Technology (Grant-in-Aid for Young Scientists (B): No. 16750046; A.I.), the Ministry of Education, Culture, Sports, Science and Technology of the Japanese Government (Grant-in-Aid for Scientific Research on Priority Areas, No. 18065009, “Chemistry of Concerto Catalysis”; M. A.), the Hayashi Memorial Foundation for Female Natural Scientists (A.I.), and the Japan Science and Technology Agency (PRESTO (Precursory Research for Embryonic Science and Technology); A.I.). We are also grateful to Dr. M. Osawa (RIKEN) for fruitful discussion.

#### References

- [1] (a) T.R. Karl, K.E. Trenberth, *Science* 302 (2003) 1719; (b) H. Akimoto, *Science* 302 (2003) 1716.
- [2] (a) N. Armaroli, B. Balzani, *Angew. Chem. Int. Ed.* 46 (2007) 52; (b) S. Licht, *Chem. Commun.* (2005) 4635; (c) S. Rau, D. Walther, J.G. Vos, *Dalton Trans.* (2007) 915; (d) A.J. Esswein, D.G. Nocera, *Chem. Rev.* 107 (2007) 40227.
- [3] (a) R.E. Blankenship, M.T. Madigan, C.E. Bauer (Eds.), *Anoxic Photosynthetic Bacteria*, Kluwer, Dordrecht, 1995; (b) D. Gust, T.A. Moore, A.L. Moore, in: V. Balzani (Ed.), *Electron Transfer in Chemistry*, vol. 3, Wiley-VCH, Weinheim, 2001, pp. 272–336.
- [4] (a) A. Collings, C. Critchley (Eds.), *Artificial Photosynthesis*, Wiley-VCH, Weinheim, 2005; (b) T. Hasobe, H. Imahori, P.V. Kamat, T.K. Ahn, S.K. Kim, D. Kim, A. Fujimoto, T. Hirakawa, S. Fukuzumi, *J. Am. Chem. Soc.* 127 (2005) 1216; (c) G. Bergamini, C. Sautan, P. Ceroni, M. Maestri, V. Balzani, M. Gorka, S.-K. Lee, J. van Heyst, F. Vögtle, *J. Am. Chem. Soc.* 126 (2004) 16466; (d) D.M. Guldi, I. Zilbermann, G. Anderson, N.A. Kotov, N. Tagmatarchis, M. Prato, *J. Am. Chem. Soc.* 126 (2004) 14340; (e) R. Konduri, N.R. de Tacconi, K. Rajeshwar, F.M. MacDonnell, *J. Am. Chem. Soc.* 126 (2004) 11621; (f) D. Gust, T.A. Moore, A.L. Moore, *Acc. Chem. Res.* 34 (2001) 40; (g) F. Fungo, A. Luis, L.A. Otero, L. Sereno, J.J. Silber, E.N. Durantini, *J. Mater. Chem.* (2000) 645; (h) C. Luo, C. Huang, L. Gan, D. Zhou, W. Xia, Q. Zhuang, Y. Zhao, Y. Huang, *J. Phys. Chem.* 100 (1996) 16685; (i) D. Gust, T.A. Moore, A.L. Moore, *Acc. Chem. Res.* 26 (1993) 198; (j) M. Nowakowska, V.P. Foyle, J.E. Guillet, *J. Am. Chem. Soc.* 115 (1993) 5975; (k) M.R. Wasielewski, *Chem. Rev.* 92 (1992) 435; (l) K. Kalyanasundaram, *Photochemistry of Polypyridine and Porphyrin Complexes*, Academic Press, London, 1992; (m) T.J. Meyer, *Acc. Chem. Res.* 22 (1989) 163.
- [5] (a) S. Fukuzumi, T. Yorisue, *Bull. Chem. Soc. Jpn.* 65 (1992) 715; (b) I. Okura, H. Hosono, *Inorg. Chim. Acta* 201 (1992) 11; (c) S. Fukuzumi, T. Kitano, M. Ishikawa, Y. Matsuda, *Chem. Phys.* 176 (1993) 337; (d) R. Sadamoto, N. Tomioka, T. Aida, *J. Am. Chem. Soc.* 118 (1996) 3978; (e) D. Curiel, K. Ohkubo, J.R. Reimers, S. Fukuzumi, M.J. Crossley, *Phys. Chem. Chem. Phys.* 9 (2007) 5260; (f) S. Fukuzumi, H. Imahori, V. Balzani (Eds.), *Electron Transfer in Chemistry*, vol. 2, 2001, p. 927; (g) J.R. Darwent, P. Douglas, A. Harriman, G. Porter, M.-C. Richoux, *Coord. Chem. Rev.* 44 (1982) 83.
- [6] (a) V. Balzani, A. Juris, M. Venturi, S. Campagna, S. Serroni, *Chem. Rev.* 96 (1996) 759 (references cited therein); (b) U.S. Schubert, C. Eschbaumer, *Angew. Chem. Int. Ed.* 41 (2002) 2892; (c) M.I.J. Polson, G.S. Hana, J.T. Nicholas, B. Hasenknopf, R. Thouvenot, *Chem. Commun.* (2004) 1314; (d) S. Weldon, L. Hammarström, E. Mukhtar, R. Hage, E. Gunneweg, J.G. Haasnoot, J. Reedijk, W.R. Browne, A.L. Guckian, J.G. Vos, *Inorg. Chem.* 43 (2004) 4471.



- (e) J.-P. Sauvage, J.-P. Collin, J.-C. Chambron, S. Guillerez, V. Balzani, F. Barigelli, L. De Cola, L. Flamigni, *Chem. Rev.* 94 (1994) 993 (references therein);  
 (f) V. Balzani, F. Scandola, *Supramolecular Photochemistry*, Horwood, Chichester, England, 1990;  
 (g) G. Denti, S. Serroni, S. Campagna, V. Ricevuto, V. Balzani, *Coord. Chem. Rev.* 111 (1991) 227;  
 (h) F. Denti, S. Campagna, L. Sabatino, S. Lerroni, M. Ciano, V. Balzani, *Inorg. Chem.* 29 (1990) 4750.
- [7] V. Balzani, A. Credi, M. Venturi, *Molecular Devices and Machines*, Chapter 5, Wiley-VCH, Weinheim, 2003.
- [8] Although oxidation by the vacant HOMO is also possible, it is not discussed in detail here for simplicity sake.
- [9] S. Takagi, H. Inoue, in: V. Ramamurthy, K.S. Schanze (Eds.), *Multimetallic and Macromolecular Inorganic Photochemistry*, Marcel Dekker, New York, 1999, pp. 215–342.
- [10] (a) S. Funiyu, T. Isobe, S. Akagi, D.A. Tryk, H. Inoue, *J. Am. Chem. Soc.* 125 (2003) 5734;  
 (b) H. Inoue, T. Okamoto, Y. Kameo, M. Sumitani, A. Fujiwara, D. Ishibashi, M. Hida, *J. Chem. Soc., Perkin Trans. 1* (1994) 105.
- [11] (a) R. Miyatani, Y. Amao, *J. Mol. Catal. B* 27 (2004) 121;  
 (b) J. Grodkowski, D. Behar, P. Neta, *J. Phys. Chem. A* 101 (1997) 248.
- [12] H. Inoue, S. Funiyu, Y. Shimada, S. Takagi, *Pure Appl. Chem.* 77 (2005) 1019.
- [13] See for example A. de Meijere, F. Diederich, *Metal-Catalyzed Cross-Coupling Reactions*, 2nd ed., Wiley, 2004;  
 E. Negishi, A. de Meijere, *Handbook of Organopalladium Chemistry for Organic Synthesis*, vols. 1 and 2, Wiley, 2002.
- [14] Back electron transfer in **D** (from LUMO of M1 to  $D^+$ ) also regenerates **A**. This process can be avoided by decomposition of  $D^+$  immediately after the electron transfer. In the case of amine, its cation radical quickly decomposes.
- [15] In case the HOMO level of RC is higher than that of PS as in **B'** (Fig. 1a') intramolecular electron transfer should form the zwitterionic species bearing a cationic charge on RC and, subsequently, analogous catalytic oxidative transformations may be feasible in the presence of a sacrificial oxidant. Because this type of examples is rare, discussion will be focused on the reductive transformations.
- [16] J.G. Vos, J.M. Kelly, *Dalton Trans.* (2006) 4869;  
 J.P. Paris, W.W. Brandt, *J. Am. Chem. Soc.* 81 (1959) 5001.
- [17] (a) A. Inagaki, S. Edure, S. Yatsuda, M. Akita, *Chem. Commun.* (2005) 5468;  
 (b) A. Inagaki, S. Yatsuda, S. Edure, A. Suzuki, T. Takahashi, M. Akita, *Inorg. Chem.* 46 (2007) 2432;  
 (c) A. Inagaki, H. Nakagawa, M. Akita, K. Inoue, M. Sakai, M. Fujii, *Dalton Trans.* (2008) 6709;  
 (d) T. Saita, H. Nitadori, A. Inagaki, M. Akita, *J. Organomet. Chem.* 694 (2009) 3125.
- [18] (a) N.S. Lewis, D.G. Nocera, *Proc. Natl. Acad. Sci. U.S.A.* 103 (2006) 15729;  
 (b) V. Balzani, A. Credi, M. Venturi, *ChemSusChem* 1 (2008) 26;  
 (c) A.F. Heyduk, D.G. Nocera, *Science* 293 (2001) 1636;  
 (d) V. Balzani, L. Moggi, M.F. Manfrin, F. Bolletta, M. Gleria, *Science* 189 (1975) 852.
- [19] (a) K. Maeda, K. Teramura, D.L. Lu, T. Takata, M. Saito, Y. Inoue, K. Domen, *Nature* 440 (2006) 295;  
 (b) K. Maeda, K. Domen, *J. Phys. Chem. C* 111 (2007) 7851;  
 (c) W.J. Youngblood, S.-H.A. Lee, Y. Kobayashi, E.A. Hernandez-Pagan, P.G. Hoertz, T.A. Moore, A.L. Moore, D. Gust, T.E. Mallouk, *J. Am. Chem. Soc.* 131 (2009) 926;  
 (d) A. Kudo, Y. Miseki, *Chem. Soc. Rev.* 38 (2009) 253.
- [20] (a) J.M. Lehn, J.P. Sauvage, *Nouv. J. Chim.* 1 (1977) 449;  
 (b) M. Kirch, J.M. Lehn, J.P. Sauvage, *Helv. Chim. Acta* 62 (1979) 1345;  
 (c) C.V. Krishnan, B.S. Brunswig, C. Creutz, N. Sutin, *J. Am. Chem. Soc.* 107 (1985) 2005;  
 (d) E. Borgarello, J. Kiwi, E. Pelizzetti, M. Visca, M. Grätzel, *J. Am. Chem. Soc.* 103 (1981) 6324;  
 (e) M. Grätzel, *Acc. Chem. Res.* 14 (1981) 376.
- [21] The electron transfer process for this system is different from others. At the stage of **C** (Scheme 3), the excited electron is transferred to  $[Rh(bipy)_3]^{3+}$  (M2) to form  $[Ru(bipy)_3]^{3+}$  and  $[Rh(bipy)_3]^{2+}$ . The former species is reduced to TB by the sacrificial electron donor, and the latter causes reduction of  $H^+$  to produce  $H_2$ .
- [22] A mechanism involving  $H_2$ -production on the Rh component as well as on colloidal Pt was proposed.
- [23] A. Magnuson, M. Anderlund, O. Johansson, P. Lindblad, R. Lomoth, T. Polivka, S. Ott, K. Stensjö, S. Styring, V. Sundström, L. Hammarström, *Acc. Chem. Res.* (2009), doi:10.1021/ar900127h.
- [24] (a) X. Hu, B.S. Brunswig, J.C. Peters, *J. Am. Chem. Soc.* 129 (2007) 8988;  
 (b) A.D. Wilson, R.H. Newell, M.J. McNevin, J.T. Muckerman, M.R. DuBois, D.L. DuBois, *J. Am. Chem. Soc.* 128 (2006) 358;  
 (c) A. Esswein, D.G. Nocera, *Chem. Rev.* 107 (2007) 4022;  
 (d) I. Okura, N. Kim-Thuan, *J. Mol. Catal.* 5 (1979) 311;  
 (e) K. Sakai, K. Matsumoto, *J. Coord. Chem.* 18 (1988) 169;  
 (f) K. Sakai, K. Matsumoto, *J. Mol. Catal.* 62 (1990) 1;  
 (g) K. Sakai, Y. Kizaki, T. Tsubomura, K. Matsumoto, *J. Mol. Catal.* 79 (1993) 141.
- [25] (a) J.I. Goldsmith, W.R. Hudson, M.S. Lowry, T.H. Anderson, S. Bernhard, *J. Am. Chem. Soc.* 127 (2005) 7502;  
 (b) E.D. Cline, S.E. Adamson, S. Bernhard, *Inorg. Chem.* 47 (2008) 10378;  
 (c) T. Lazarides, T. McCormick, P. Du, G. Luo, B. Lindley, R. Eisenberg, *J. Am. Chem. Soc.* 131 (2009) 9192;
- (d) P. Du, K. Knowles, R. Eisenberg, *J. Am. Chem. Soc.* 130 (2008) 12576;  
 (e) P. Du, J. Schneider, F. Li, W. Zhao, U. Patel, F.N. Castellano, R. Eisenberg, *J. Am. Chem. Soc.* 130 (2008) 5056;  
 (f) J. Zhang, P. Du, J. Schneider, P. Jarosz, R. Eisenberg, *J. Am. Chem. Soc.* 129 (2007) 7726;  
 (g) Y. Na, M. Wang, J. Pan, P. Zhang, B. Åkermark, L. Sun, *Inorg. Chem.* 47 (2008) 2805.
- [26] (a) H. Ozawa, M. Haga, K. Sakai, *J. Am. Chem. Soc.* 128 (2006) 4926;  
 (b) H. Ozawa, Y. Yokoyama, M. Haga, K. Sakai, *Dalton Trans.* (2007) 1197;  
 (c) H. Ozawa, K. Sakai, *Chem. Lett.* 36 (2007) 920;  
 (d) K. Sakai, H. Ozawa, *Coord. Chem. Rev.* 251 (2007) 2753.
- [27] S. Rau, B. Schäfer, D. Gleich, E. Anders, M. Rudolph, M. Friedrich, H. Görls, W. Henry, J.G. Vos, *Angew. Chem. Int. Ed.* 45 (2006) 6215.
- [28] P. Lei, M. Hedlund, R. Lomoth, H. Rensmo, O. Johansson, L. Hammarström, *J. Am. Chem. Soc.* 130 (2008) 26.
- [29] (a) S.M. Arachchige, J.R. Brown, E. Chang, A. Jain, D.F. Zigler, K. Rangan, K. Brewer, *Inorg. Chem.* 48 (2009) 1989;  
 (b) M. Elvington, J. Brown, S.M. Arachchige, K.J. Brewer, *J. Am. Chem. Soc.* 129 (2007) 10644.
- [30] A. Fihri, V. Artero, M. Razavet, C. Baffert, W. Leibl, M. Fontecave, *Angew. Chem. Int. Ed.* 47 (2008) 564.
- [31] Y. Miyake, K. Nakajima, K. Sasaki, R. Saito, H. Nakanishi, Y. Nishibayashi, *Organometallics* 28 (2009) 5240.
- [32] S. Tschierlei, M. Presselt, C. Kuhnt, A. Yartsev, T. Pascher, V. Sundström, M. Karnahl, M. Schwalbe, B. Schäfer, S. Rau, M. Schmitt, B. Dietzek, J. Popp, *Chem. Eur. J.* 15 (2009) 7678.
- [33] T. Sakakura, J.-C. Choi, H. Yasuda, *Chem. Rev.* 107 (2007) 2365.
- [34] (a) A. Correa, R. Martin, *Angew. Chem. Int. Ed.* 48 (2009) 6201;  
 (b) X. Yin, J.R. Moss, *Coord. Chem. Rev.* 181 (1999) 27.
- [35] (a) H. Ishida, K. Tanaka, T. Tanaka, *Chem. Lett.* (1987) 1035;  
 (b) S. Matsuoka, T. Kohzaki, C. Pac, A. Ishida, S. Takamuku, M. Kusaba, N. Nakashima, S. Yanagida, *J. Phys. Chem.* 96 (1992) 4437.
- [36] B.R. Eggins, J.T.S. Irvine, E.P. Murphy, J. Grimshaw, *J. Chem. Soc., Chem. Commun.* (1988) 1123.
- [37] M. Komatsu, T. Aida, S. Inoue, *J. Am. Chem. Soc.* 113 (1991) 8492.
- [38] (a) J. Hawecker, J.-M. Lehn, R. Ziessel, *J. Chem. Soc., Chem. Commun.* (1985) 56;  
 (b) I. Wilner, D. Mandler, *J. Am. Chem. Soc.* 111 (1989) 1330.
- [39] R. Maidan, I. Willner, *J. Am. Chem. Soc.* 108 (1986) 8100.
- [40] (a) J. Hawecker, J.-M. Lehn, R. Ziessel, *J. Chem. Soc. Chem. Commun.* (1983) 536;  
 (b) J. Hawecker, J.-M. Lehn, R. Ziessel, *Helv. Chim. Acta* 69 (1986) 536;  
 (c) J.L. Grant, K. Goswami, L.O. Spreer, J.W. Otvos, M. Calvin, *J. Chem. Soc., Dalton Trans.* (1987) 2105;  
 (d) E. Kimura, X. Bu, M. Shionoya, S. Wada, S. Maruyama, *Inorg. Chem.* 31 (1992) 4542;  
 (e) O. Ishitani, M.W. George, T. Ibusuki, F.P.A. Johnson, K. Koike, K. Nozaki, C. Pac, J.J. Turner, J.R. Westwell, *Inorg. Chem.* 33 (1994) 4712;  
 (f) T. Ogata, S. Yanagida, B.S. Brunswig, E. Fujita, *Energy Convers. Manage.* 36 (1995) 669;  
 (g) T. Ogata, Y. Yamamoto, Y. Wada, K. Murakoshi, M. Kusaba, N. Nakashima, A. Ishida, S. Takamuku, S. Yanagida, *J. Phys. Chem.* 99 (1995) 11916.
- [41] (a) A.T.A. Tinnermans, T.P.M. Koster, D.H.M.W. Thewessen, A. Mackor, *Recl. Trav. Chim. Pays. Bas.* 103 (1984) 288;  
 (b) J.L. Grant, K. Goswami, L.O. Spreer, J.W. Otvos, M. Calvin, *J. Chem. Soc., Dalton Trans.* (1987) 2105;  
 (c) C.A. Craig, L.O. Spreer, J.W. Otvos, M. Calvin, *J. Phys. Chem.* 94 (1990) 7957.
- [42] (a) K. Koike, H. Hori, M. Ishizuka, J.R. Westwell, K. Takeuchi, T. Ibusuki, K. Enjouji, H. Konno, K. Sakamoto, O. Ishitani, *Organometallics* 16 (1997) 5724;  
 (b) H. Hori, F.P.A. Johnson, K. Koike, O. Ishitani, T. Ibusuki, *J. Photochem. Photobiol. A* 96 (1996) 171.
- [43] H. Takeda, K. Koike, H. Inoue, O. Ishitani, *J. Am. Chem. Soc.* 130 (2008) 2023.
- [44] (a) E. Kimura, X. Bu, M. Shionoya, S. Wada, S. Maruyama, *Inorg. Chem.* 31 (1992) 4542;  
 (b) E. Kimura, S. Wada, M. Shionoya, Y. Okazaki, *Inorg. Chem.* 33 (1994) 770;  
 (c) E. Kimura, S. Wada, M. Shionoya, T. Takahashi, Y. Iitaka, *J. Chem. Soc., Chem. Commun.* (1990) 397.
- [45] (a) B. Gholamkhash, H. Mametsuka, K. Koike, T. Tanabe, M. Furue, O. Ishitani, *Inorg. Chem.* 44 (2005) 2326;  
 (b) Z.-Y. Bian, K. Sumi, M. Furue, S. Sato, K. Koike, O. Ishitani, *Inorg. Chem.* 47 (2008) 10801.
- [46] Mononuclear Re species show catalytic activity, as is consistent with the reports by Ziessel and Lehn [38] and Ishitani and coworkers [43].
- [47] M. Osawa, H. Nagai, M. Akita, *Dalton Trans.* (2007) 827.
- [48] K. Sonogashira, Y. Tohda, N. Hagihara, *Tetrahedron Lett.* (1975) 4467;  
 R. Chinchilla, C. Najera, *Chem. Rev.* 107 (2007) 874;  
 H. Doucet, J.-C. Hierso, *Angew. Chem. Int. Ed.* 46 (2007) 834.
- [49] M. Osawa, M. Akita, unpublished results.
- [50] (a) D.A. Nicewicz, D.W.C. MacMillan, *Science* 322 (2008) 77;  
 (b) D.A. Nagib, M.E. Scott, D.W.C. MacMillan, *J. Am. Chem. Soc.* 131 (2009) 10875.
- [51] T. Koike, M. Akita, *Chem. Lett.* 38 (2009) 166.
- [52] Related reductive transformations of enones giving [2+2]-cycloaddition products were recently reported by Yoon. The reduced TB(1)+ species first undergoes SET to enone to form an anion radical intermediate, which attacks another enone molecule via a Michael addition-like mechanism finally to give the cycloaddition product;

- (a) M.A. Isehay, M.E. Anzovino, D.J. Du, T.P. Yoon, *J. Am. Chem. Soc.* 130 (2008) 12886;  
(b) J. Du, T.P. Yoon, *J. Am. Chem. Soc.* 131 (2009) 14604;  
(c) See also J.M. Narayanam, J.W. Tucker, C.R.J. Stephenson, *J. Am. Chem. Soc.* 131 (2009) 8756.
- [53] M. Osawa, M. Hoshino, Y. Wakatsuki, *Angew. Chem. Int. Ed.* 40 (2001) 3472.
- [54] (a) V. Balzani, A. Juris, M. Venturi, S. Campagna, S. Serroni, *Chem. Rev.* 96 (1996) 759;  
(b) P.F.H. Schwab, M.D. Levin, J. Michl, *Chem. Rev.* 99 (1999) 1863;  
(c) L. Flamigni, F. Barigelletti, M. Armaroli, B. Ventura, J.-P. Collin, J.-P. Sauvage, J.A.G. Williams, *Inorg. Chem.* 38 (1999) 661;  
(d) S. Encina, A.M. Barthram, M.D. Ward, F. Barigelletti, S. Campagna, *Chem. Commun.* (2001) 277;  
(e) M. Kercher, B. König, H. Zieg, L. De Cola, *J. Am. Chem. Soc.* 124 (2002) 11541;  
(f) P.P. Lainé, F. Bedioui, F. Loiseau, C. Chiorboli, S. Campagna, *J. Am. Chem. Soc.* 128 (2006) 7510;  
(g) T. Lazarides, A. Barbieri, C. Sabatini, F. Barigelletti, H. Adams, M.D. Ward, *Inorg. Chim. Acta* 360 (2007) 814;  
(h) B. Ventura, A. Barbieri, F. Barigelletti, J.B. Seneclauze, P. Ratailleau, R. Ziessel, *Inorg. Chem.* 47 (2008) 7048.
- [55] V.W.-W. Yam, V.W.-M. Lee, K.-K. Cheung, *Organometallics* 16 (1997) 2833.
- [56] A. Juris, V. Balzani, F. Barigelletti, S. Campagna, P. Belser, A. Von Zelewsky, *Cood. Chem. Rev.* 85 (1988) 85.
- [57] E. Bulak, M. Leboschka, B. Schwederski, O. Sarper, T. Varnali, J. Fiedler, F. Lissner, T. Schleid, W. Kaim, *Inorg. Chem.* 46 (2007) 5562;  
Data for N-coordinated Pd(II) species are few presumably because of lack of reversible redox processes. 'd(II) species coordinated by less electron-withdrawing S ligands generally show redox processes in more negative side (−0.65 to −1.71 V);  
See, for example A.J. Blake, G. Reid, M. Schröder, *J. Chem. Soc., Dalton Trans.* (1990) 3363;  
G.A. Bowmaker, P.D.W. Boyd, G.K. Campbell, M. Zvagulis, *J. Chem. Soc., Dalton Trans.* (1986) 1065;  
G.J. Grant, D.F. Galas, M.W. Jones, K.D. Loveday, W.T. Pennington, G.L. Schimek, C.T. Eagle, D.G. VanDerveer, *Inorg. Chem.* 37 (1998) 5299;  
T. Tuntulani, G. Musie, J.H. Reibenspies, M.Y. Darensbourg, *Inorg. Chem.* 34 (1995) 6279;  
G.J. Grant, S.M. Carer, A.L. Russel, I.M. Poullaos, D.G. VanDerveer, *J. Organomet. Chem.* 637–639 (2001) 683.
- [58] L.K. Johnson, C.M. Killian, M. Brookhart, *J. Am. Chem. Soc.* 117 (1995) 6414;  
W. Liu, M. Brookhart, *Organometallics* 23 (2004) 6099.
- [59] (a) Y. Yamamoto, M. Irie, Y. Yamamoto, K. Hayashi, *J. Chem. Soc., Perkin Trans. II* (1979) 1517;  
(b) B. Chaudhuri, M.M. Sharma, *Ind. Eng. Chem. Res.* 28 (1989) 1757;  
(c) A. Heidekum, M. Harmer, W.F. Holderich, *Catal. Lett.* 47 (1997) 243;  
(d) Q. Sun, W.E. Farneth, M.A. Harmer, *J. Catal.* 164 (1996) 62;  
(e) B. Chaudhuri, *Org. Proc. Res. Dev.* 3 (1999) 220.
- [60] S. Sakaki, H. Mizutani, Y. Kase, *Inorg. Chem.* 31 (1992) 4575.